

**University of Alberta**

**The Use of Polyacrylamide as a Selective Depressant in the Separation  
of Chalcopyrite and Galena**

by

**Lei Wang**

A thesis submitted to the Faculty of Graduate Studies and Research  
in partial fulfillment of the requirements for the degree of

**Master of Science**  
in  
**Materials Engineering**

Department of Chemical and Materials Engineering

©Lei Wang  
Spring 2013  
Edmonton, Alberta

Permission is hereby granted to the University of Alberta Libraries to reproduce single copies of this thesis and to lend or sell such copies for private, scholarly or scientific research purposes only. Where the thesis is converted to, or otherwise made available in digital form, the University of Alberta will advise potential users of the thesis of these terms.

The author reserves all other publication and other rights in association with the copyright in the thesis and, except as herein before provided, neither the thesis nor any substantial portion thereof may be printed or otherwise reproduced in any material form whatsoever without the author's prior written permission.

## **ABSTRACT**

High molecular weight polyacrylamide (PAM) was tested as a potential selective depressant in the differential flotation separation of galena and chalcopyrite using potassium ethyl xanthate (KEX) as a collector. In single mineral flotation, PAM depressed chalcopyrite while galena was floatable. Mechanism study indicated that PAM could adsorb on galena through hydrogen bonding, and on chalcopyrite through hydrogen bonding as well as ammonium-copper complexation. KEX could only break up the galena-PAM bonding. It is the combined use of PAM and KEX that caused the selectivity.

In mineral mixture flotation, galena and chalcopyrite could be separated by PAM and KEX only after EDTA treatment of the mineral mixtures. Time of flight secondary ion mass spectrometric (ToF-SIMS) measurements indicated that when galena and chalcopyrite were present together in the suspension, PAM adsorbed on both galena and chalcopyrite. However, after prior treatment of the mineral mixture by EDTA, PAM mainly adsorbed on chalcopyrite.

## **ACKNOWLEDGEMENT**

First and foremost, I would like to express my deepest gratitude to my supervisor, Dr. Qi Liu, for his guidance, patience and encouragement throughout the project. I really have learned a lot from his invaluable guidance during the past two and half years. It has been my great honor to be his student.

The financial support provided by Canadian Center for Clean Coal/Carbon and Mineral Processing Technology (C<sup>5</sup>MPT) is gratefully acknowledged.

During the course of this project, Dr. Mingli Cao, Dr. Anqiang He, Dr. Shihong Xu (ACSES) and Mr. Shiraz Merali have helped me with the testwork, which I really appreciate.

Last but not the least, I am indeed grateful to all my group members, Dr. Kaipeng Wang, Dr. Min Tang, Ph.D. students Jihua Gong, Xiao Ni and Peng Huang, M.Sc. students Marc Parrent and Huiran Wang, for their friendship and encouragement.

## Table of Contents

1. INTRODUCTION .....	1
2. LITERATURE REVIEW .....	4
2.1 Froth Flotation.....	4
2.2 Differential Flotation of Galena and Chalcopyrite .....	7
2.3 Challenges Associated With Fine Particle Flotation.....	9
2.4 Polyacrylamide (PAM) .....	12
2.4.1 <i>Introduction of Polyacrylamide</i> .....	12
2.4.2 <i>Previous Research of PAM as Depressant in Flotation</i> .....	14
2.4.3 <i>Adsorption Mechanism of PAM on Mineral Surface</i> .....	16
2.5 Surface Contamination by Metal Ions and EDTA Extraction.....	19
3. RESEARCH OBJECTIVES .....	21
4. EXPERIMENTAL MATERIALS AND METHODS .....	22
4.1 Materials and Reagents .....	22
4.2 Experimental Procedure .....	23
4.2.1 <i>Froth flotation</i> .....	23
4.2.2 <i>Contact Angle Measurements</i> .....	25
4.2.3 <i>Zeta Potential Measurements</i> .....	26

4.2.4 X-Ray Element Mapping Measurements .....	28
4.2.5 ToF-SIMS Measurements .....	29
4.2.6 XPS Measurements .....	30
5. RESULTS AND DISCUSSION .....	33
5.1 Single Sulfide Mineral Flotation .....	33
5.2 Adsorption Mechanism of PAM on Galena and Chalcopyrite .....	36
5.2.1 Zeta Potential Measurement .....	36
5.2.2 Contact Angle Measurement .....	38
5.2.3 XPS Measurement .....	40
5.3 Galena and Chalcopyrite Mixture Flotation .....	52
5.3.1 Galena and Chalcopyrite Mixture Flotation without Surface Cleaning .....	52
5.3.2 X-ray Element Mapping Measurements .....	54
5.3.3 The Use of EDTA for Surface Cleaning .....	56
5.3.4 Galena and Chalcopyrite Mixture Flotation with EDTA as a Cleaning Agent .....	58
5.3.5 ToF-SIMS Measurements .....	61
6. CONCLUSIONS AND RECOMMENDATIONS .....	65

6.1 General Findings .....	65
6.2 Recommendations for Future Work .....	67
<b>BIBLIOGRAPHY .....</b>	<b>69</b>

## **List of Tables**

Table 5.1 Binding energy and relative intensity of N 1s peaks of polyacrylamide, and galena and chalcopryrite with PAM or with PAM and KEX .....	51
---	----

## List of Figures

Figure 2.1 Schematics of froth flotation process (Webster's-online-dictionary) ....	5
Figure 2.2 Mineral recovery after 6.5 minutes of flotation of a polymetallic ore from Eastern Canada. Cp – chalcopyrite; Sp – sphalerite; Ga – galena; Py – pyrite; NMG – non-metallic gangue. (Liu, 2012) .....	10
Figure 2.3 Structure unit of PAM (Sojka and Lentz, 1994) .....	12
Figure 2.4 Examples of typical acrylamide based monomers (Moody, 1992) .....	14
Figure 4.1 Small scale-flotation tube .....	24
Figure 4.2 Krüss DSA 10 Mk2 drop shape contact angle measuring instrument.	26
Figure 4.3 ZetaPALS Zeta Potential Analyzer. ....	28
Figure 4.4 ToF-SIMS IV - 100 spectrometer (ION-TOF GmbH).....	30
Figure 4.5 Axis 165 X-ray Photoelectron Spectrometer (Kratos Analytical). ....	32
Figure 5.1 Recovery of single sulfide mineral flotation as a function of pH in the absence of PAM as depressant. (KEX: $5 \times 10^{-4}$ mol/L; Condition time: 3 min; Flotation time: 5 min). ....	33
Figure 5.2 Recovery of single sulfide mineral flotation as a function of pH in the presence of PAM as a depressant. (PAM: 8 mg/L; KEX: $5 \times 10^{-4}$ mol/L; Condition time: 3 min; Flotation time: 5 min). ....	35
Figure 5.3 Zeta potential versus pH for galena and chalcopyrite conditioned in 0.01 mol/L KCl solution, with and without PAM. ....	37
Figure 5.4 The contact angle images of a water sessile drop on the pressed pellet	



of (a) galena, (b) galena after PAM adsorption, (c) galena after PAM and KEX adsorption, (d) chalcopyrite, (e) chalcopyrite after PAM adsorption, (f) chalcopyrite after PAM and KEX adsorption. (pH = 10; PAM: 8 mg/L; KEX:  $5 \times 10^{-4}$  mol/L; pellet press pressure: 5000 psi.) . 39

Figure 5.5 XPS spectra of PAM by (a) survey scan, (b) N 1s narrow scan. .... 42

Figure 5.6 XPS spectra of N 1s narrow scan for (a) galena, (b) chalcopyrite. .... 43

Figure 5.7 XPS spectra of N 1s narrow scan for (a) galena after PAM treatment, (b) chalcopyrite after PAM treatment..... 47

Figure 5.8 XPS spectra of N 1s narrow scan for (a) galena after PAM and KEX treatment, (b) chalcopyrite after PAM and KEX treatment..... 50

Figure 5.9 Recovery of the mixture of chalcopyrite and galena (weight ratio 1:1) flotation as a function of PAM dosage. (KEX:  $5 \times 10^{-4}$  mol/L; Condition time: 3 min; Flotation time: 5 min). .... 53

Figure 5.10 Energy-dispersive X-ray element mapping images of galena and chalcopyrite mixture: (a) grain BSE image of the mineral sample, (b) lead element mapping image, (c) copper element mapping image. .... 55

Figure 5.11 Copper ion concentration released from galena samples contacted with chalcopyrite, before and after EDTA treatment..... 57

Figure 5.12 Flotation of chalcopyrite and galena mixture (weight ratio 1:1) with EDTA as a function of pH. (a) Metal recovery in froth product; (b) Metal grade in froth product. (EDTA: 20 mg/L; PAM: 8 mg/L; KEX:

$5 \times 10^{-4}$  mol/L; Flotation time: 5 min). ..... 59

Figure 5.13 Flotation of the mixture of chalcopyrite and galena with EDTA as a function of EDTA dosage. (pH 10; PAM: 8 mg/L; KEX:  $5 \times 10^{-4}$  mol/L; Flotation time: 5 min)..... 60

Figure 5.14 ToF-SIMS images  $50 \mu\text{m} \times 50 \mu\text{m}$  region of the surface of a mixture of chalcopyrite and galena after PAM and KEX treatment. (a) Image of chalcopyrite ( $\text{Cu}^+$ ); (b) Image of galena ( $\text{Pb}^+$ ); (c) Image of PAM ( $\text{C}_3\text{H}_5\text{ON}$ ). ..... 62

Figure 5.15 ToF-SIMS images of  $50 \mu\text{m} \times 50 \mu\text{m}$  region of the surface of a mixture of chalcopyrite and galena after EDTA cleaning and PAM and KEX treatment. (a) Image of chalcopyrite ( $\text{Cu}^+$ ); (b) Image of galena ( $\text{Pb}^+$ ); (c) Image of PAM ( $\text{C}_3\text{H}_5\text{ON}$ )..... 64

## **1. INTRODUCTION**

Sulfide ores are the major sources of base metals such as copper, lead, zinc, nickel, etc. In most cases, lead-copper-zinc sulfide ores are grouped together in the deposits. In mineral processing industry, inorganic depressants such as sodium cyanide, potassium dichromate, sulfur dioxide, are routinely used in differential sulfide flotation (i.e., to separate the sulfide minerals from each other). One obvious disadvantage of these inorganic depressants is that they are toxic and hazardous, and not environment friendly. In addition, they cannot truly depress the fine and ultrafine sulfide minerals due to the propensity of these particles to mechanically entrain into flotation concentrate, although the inorganic depressants may render the fine and ultrafine particles completely hydrophilic.

Therefore, it is proposed that non-toxic high molecular weight polymeric depressants should be developed and used in differential sulfide flotation, not only to replace the toxic inorganic depressants but also to lower the entrainment of the fine and ultrafine mineral particles. This concept has been verified by the recent work of Liu et al. (2006) who showed that, in the flotation of several oxide minerals including iron oxide, hydroxyapatite, and quartz, the use of high molecular weight selective polymeric flotation depressants could flocculate the

fine and ultrafine particles as well as render them hydrophilic, thus lowering both the flotation and mechanical entrainment of the minerals that are to be depressed.

In the present study, polyacrylamide (PAM) with a high molecular weight has been chosen as the “dual functional” polymer depressant. PAM, as a widely commercially used polymer in many industries, has proven its effectiveness as a flocculant in mineral processing industry by previous research. Thus, our study focuses on the selective depressive effect of PAM on Cu-Pb sulfide flotation, which has never been studied before.

The purpose of the experimental work carried out in the thesis project is to determine if PAM possesses unique selectivity in galena and chalcopyrite single mineral flotation, and if it can separate these two sulfide minerals in their mixture flotation. Meanwhile, the adsorption mechanism of PAM on galena and chalcopyrite will be studied by several surface analysis techniques, to understand the phenomenon observed in flotation tests.

In the thesis that follows, Chapter 2 contains a literature review which presents a general background of Cu-Pb differential flotation and the use of PAM. Chapter 3 describes the objectives of the research project. Chapter 4 describes the experimental procedures and testing materials. Chapter 5 presents the major results from the experimental work together with discussions of the results, which

are followed by Chapter 6 presenting the conclusions of the present study and recommendations for future work.

## **2. LITERATURE REVIEW**

### **2.1 Froth Flotation**

Mineral processing is the process of separating commercially valuable minerals from their raw ores. The separation processes utilize the differences in the physical or chemical properties of the minerals, such as particle size, density, electrical and magnetic properties, and surface wettability.

Froth flotation is a process to selectively separate value minerals from gangue minerals by taking advantage of differences of their surface wettability. Unlike other physical properties, surface wettability can be readily modified with flotation collectors and modifiers. Therefore, the flotation process has been widely used for the separation of almost all types of minerals and ores, and is the most important technique in mineral processing. An illustration of the basic froth flotation concept is shown in Figure 2.1. In a typical flotation process, the raw ores are first crushed and ground to reduce particle sizes to achieve a desired degree of mineral liberation. Then appropriate chemical reagents are added to the ore suspension to render the value minerals hydrophobic and gangue minerals hydrophilic. Afterwards, an air stream is introduced to the slurry from the base of the flotation cell to generate small air bubbles. Hydrophobic particles can attach to air bubbles and float to the pulp surface forming a froth layer. Hydrophilic

particles will remain in the pulp. Thus, mineral particles with different wettability are separated.

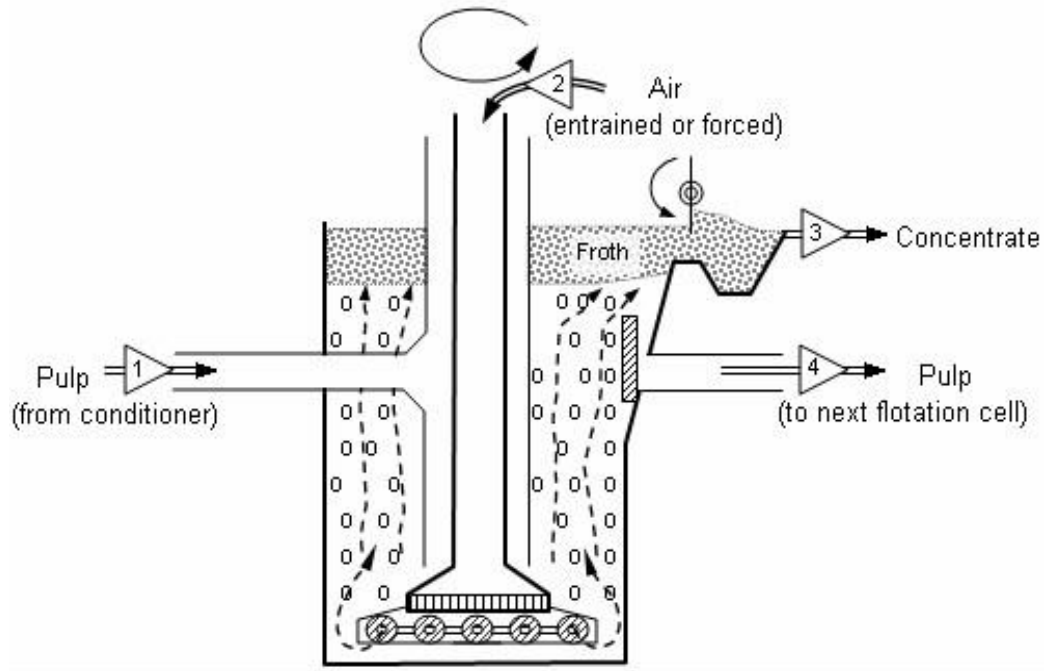


Figure 2.1 Schematics of froth flotation process (Webster's-online-dictionary)

Reagents are of great importance in froth flotation since they can modify the wettability of particle surface. Flotation reagents can be classified into three categories: collectors, frothers, and regulators (Lovell, 1982).

**Collectors** are a large group of bipolar surfactants which can selectively render the surface of mineral hydrophobic. According to their molecular structure and ion dissociation properties, collectors can be divided into ionizing collectors and non-ionizing collectors (Bulatovic, 2007). The ionizing collectors can dissociate

into ions, which can be further divided into anionic collectors and cationic collectors. In contrast, non-ionizing collectors, which are principally non-polar hydrocarbon compounds, are insoluble in water. It is believed that these collectors can form a thin film onto slightly hydrophobic mineral surface to enhance its hydrophobicity.

*Frothers* are heteropolar surface-active compounds containing a polar group, primarily -OH, and a hydrocarbon radical, capable of adsorbing at the water-air interface. They are used to provide a stable froth layer giving the floated mineral particles sufficient residence time before they are removed into flotation concentrate. Depending on the frother behavior at different pH values, the frothers can be classified into three types: Acidic frothers such as phenols, Neutral frothers such as alcohols, Basic frothers such as pyridine base (Dudenkov, 1969).

*Regulators*, or modifiers, are generally regarded as the most important reagents in mineral processing since they can control the interaction between collectors and individual minerals to ensure that the value minerals can be floated selectively. They can further be divided into three types: activators which can enhance collector attachment to value minerals, depressants which enhance the hydrophilicity of gangue minerals so that they do not float, and pH modifiers which adjust the pH of the pulp phase to an optimum condition for flotation.



## 2.2 Differential Flotation of Galena and Chalcopyrite

In general, there are two basic approaches to achieve copper-lead sulfide mineral separation: to depress copper sulfide and float lead sulfide, or to depress lead sulfide and float copper sulfide (Bulatovic, 2007). In industry, a bulk copper sulfide and lead sulfide concentrate is usually floated first, followed by the Cu-Pb separation using one of the two approaches. When copper sulfide is the major component (i.e., more copper sulfide than lead sulfide), sodium cyanide (NaCN) is usually used to depress copper sulfide. Depending on different copper-lead bulk concentration composition, different combinations of NaCN, KCN and Na<sub>2</sub>S, Na<sub>2</sub>SO<sub>3</sub> are used. The method of depressing lead sulfide while floating copper sulfide is normally used when the ratio of Cu and Pb is less than unity or when the bulk concentrate is not sufficiently clean to produce a final copper and lead concentrate after separation. These depressants for lead sulfide include dichromate alone or with lime or SO<sub>2</sub>, sulfoxo compounds with or without oxidants, and SO<sub>2</sub>/starch with or without heating (McQuiston, 1957; Roberts et al., 1980; Shimoiizaka, 1976).

Beside the inorganic depressants above which are mostly toxic, some organic depressants have been shown to be the effective alternatives. Schnarr (1978) reported that dextrin together with SO<sub>2</sub> depressed galena in Brunswick Mines in

Canada. Allan and Bourke (1978) reported that guar gum together with SO<sub>2</sub> at pH 4 depressed galena in Matabi Mines. Liu (1982) observed that carboxymethyl cellulose (CMC) depressed galena when used together with pyrophosphate in laboratory tests. Another case using sodium pyrophosphate as depressant is from Qin et al. (2012). They reported that the separation could be achieved within the pH range from 2.5 to 6 using sodium pyrophosphate to depress galena but not chalcopyrite when *O*-isopropyl-*N*-ethyl thionocarbamate (IPETC) was used as the collector.

Lin and Burdick (1988) studied the Cu-Pb separation process by using a combination of various guar gums (or starches) and sulfurous acid. The results showed that, to selectively depress galena, sulfonated guar was the most effective, followed by a low molecular weight carboxymethyl guar, un-substituted guar gum and finally, corn starch.

In Liu and Laskowski's study of dextrin in the separation of galena and chalcopyrite (Liu and Laskowski, 1989b), the separation was achieved in two pH regions: around pH 6, chalcopyrite was depressed while galena could be floated when dextrin was added prior to xanthate; around pH 12, galena was depressed while chalcopyrite could be floated when dextrin was added after xanthate.

In a recent study by using chitosan in differential flotation of Cu-Pb sulfides (Huang et al., 2012a), it is interesting to see that although chitosan depressed both galena and chalcopyrite in single mineral flotation, it could selectively depress chalcopyrite while galena was floated at pH 4 in the mineral mixture flotation.

### **2.3 Challenges Associated With Fine Particle Flotation**

The separation of fine and ultrafine mineral particles by froth flotation is a challenge to the whole mineral processing industry. With the depletion of high grade ores that are more easily processed, the minerals industry has had to deal with ores of an increasingly lower grade and more complex dissemination. As a result, ultrafine grinding is required to achieve mineral liberation, which generates large amount of fine and ultrafine particles. These particles possess small masses and high specific surface areas, and cause two major problems in froth flotation: the slow flotation rate of hydrophobic particles and the mechanical entrainment of hydrophilic particles (Trahar, 1981; Trahar and Warren, 1976). The slow flotation rate leads to the low recovery of the hydrophobic particles, resulting in the loss of value minerals to tailings. Mechanical entrainment is believed to happen when particle size is below about 30  $\mu\text{m}$ , and becomes predominant when below 10  $\mu\text{m}$  (Johnson, 1974; Trahar, 1981; L.J. Warren, 1984). The problem associated with mechanical entrainment is that it is non-selective with no distinction between hydrophobic and hydrophilic particles. The grade of concentrate is lowered when

fine and ultrafine gangue mineral particles entrain into the froth product. For example, Figure 2.2 shows the Cu-Pb bulk rougher flotation recovery of a polymetallic sulfide ore from Eastern Canada after 6.5 min of flotation. As can be seen, when particle sizes were below about 20  $\mu\text{m}$ , the recoveries of galena and chalcopyrite dropped, while the recoveries of sphalerite and pyrite, as well as non-metallic gangue increased significantly.

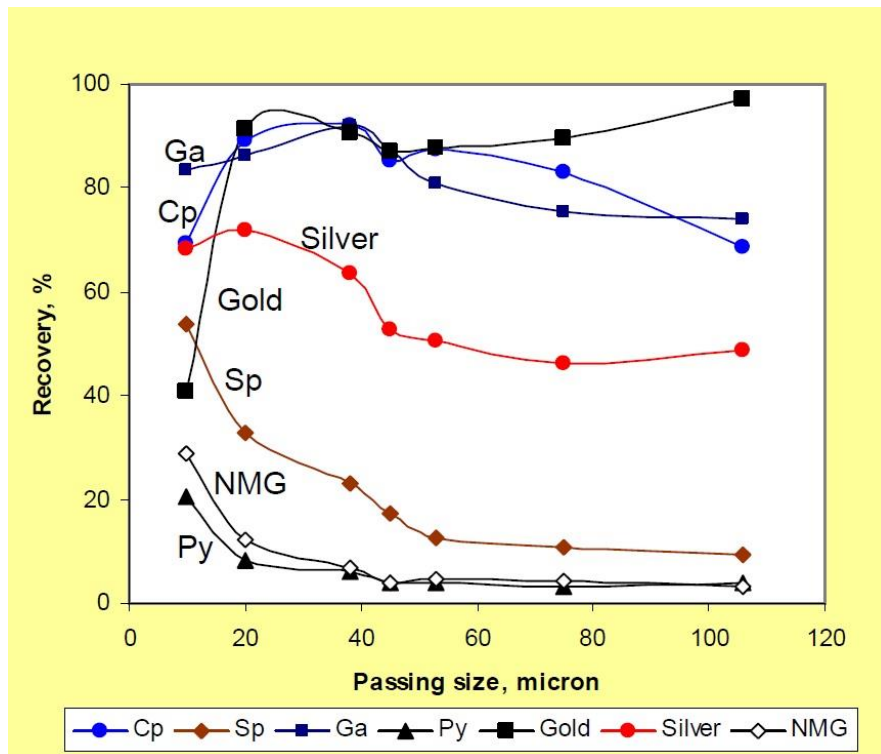


Figure 2.2 Mineral recovery after 6.5 minutes of flotation of a polymetallic ore from Eastern Canada. Cp – chalcopyrite; Sp – sphalerite; Ga – galena; Py – pyrite; NMG – non-metallic gangue. (Liu, 2012)

Several techniques have been tested to improve the flotation recovery of ultrafine hydrophobic particles. These techniques have been reviewed by Sivamohan (1990), Subrahmanyam and Forssberg (1990) and Singh et al. (1997). The main reason for the low recovery is the inefficient collision between the fine and ultrafine particles with the gas bubbles due to the small masses and sizes of the particles. Therefore most techniques proposed are aimed at improving the collision efficiency either by increasing the collision possibility, and/or subsequent adhesion following the collision. These techniques include flocculation (Song et al., 2001; Leonard J. Warren, 1975), spherical agglomeration (Cebeci, 2003; Sönmez and Cebeci, 2003), carrier flotation (Rubio and Hoberg, 1993), micro-bubble flotation (Ahmed and Jameson, 1985; Neethling and Cilliers, 2001), and use of chemisorbing flotation collector (M. C. Fuerstenau et al., 1970). These techniques can improve the recovery of fine hydrophobic particles to different degrees. However, one common problem for these techniques is that fine hydrophilic gangue mineral particles are kept highly dispersed throughout the flotation process, which can still entrain into the flotation concentrate.

## 2.4 Polyacrylamide (PAM)

### 2.4.1 Introduction of Polyacrylamide

Polyacrylamide, with a general chemical formula  $(-\text{CH}_2\text{CHCONH}_2-)$ , is a water-soluble synthetic organic polymer (Seybold, 1994). Polyacrylamide has various other names including polyacrylicamide, poly(1-carbamoylethylene) or poly(2-propenamide) (IUPAC); and acronyms including PAam, PAM (Daughton, 1988). It is formed with acrylamide subunits and its structure is shown in Figure 2.3. As can be seen, the major functional group in PAM is amide group. PAM can be formulated with copolymers to give specific charges; the molecular weight can also be manipulated and generally range from a few thousand to more than 10 million. Both molecular weights and charges give PAM its various characteristics (Green and Stott, 1999).

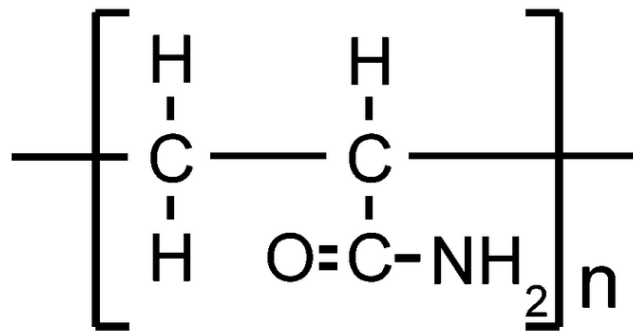


Figure 2.3 Structure unit of PAM (Sojka and Lentz, 1994)

There are three types of PAM in term of charge: non-ionic PAM, cationic PAM and anionic PAM. Non-ionic PAM is a homo-polymer of acrylamide units. Cationic and anionic PAMs are produced by copolymerization of acrylamide and a suitable cationic or anionic co-monomer or by one of a variety of post-polymerization reaction sequences starting with acrylamide homo-polymer (Mortimer, 1991). Some typical non-ionic, anionic and cationic acrylamide based monomers are shown in Figure 2.4. Non-ionic PAMs are mainly employed as flocculants in solid-liquid separation in water treatment and mineral processing industry. Cationic PAMs are particularly useful for flocculation of sewage sludge and various industrial wastes, as well as retention aids in the paper industry. Anionic PAMs are widely used in many industries, such as water treatment, paper making, mineral and coal processing, petroleum production, and food processing (Barvenik, 1994; Lipp and Kozakiewicz, 1991; Mortimer, 1991).

PAM can be modified into various derivatives to achieve desired characteristics, basically in two ways. One is the transformation into ionic polymers, which can enhance its hydrophobicity and solubility such as hydrolysis; the other one is the synthesis of graft copolymers such as starch or inorganic molecule such as carboxyl group (Boulton et al., 2001; Zhang et al, 2004).

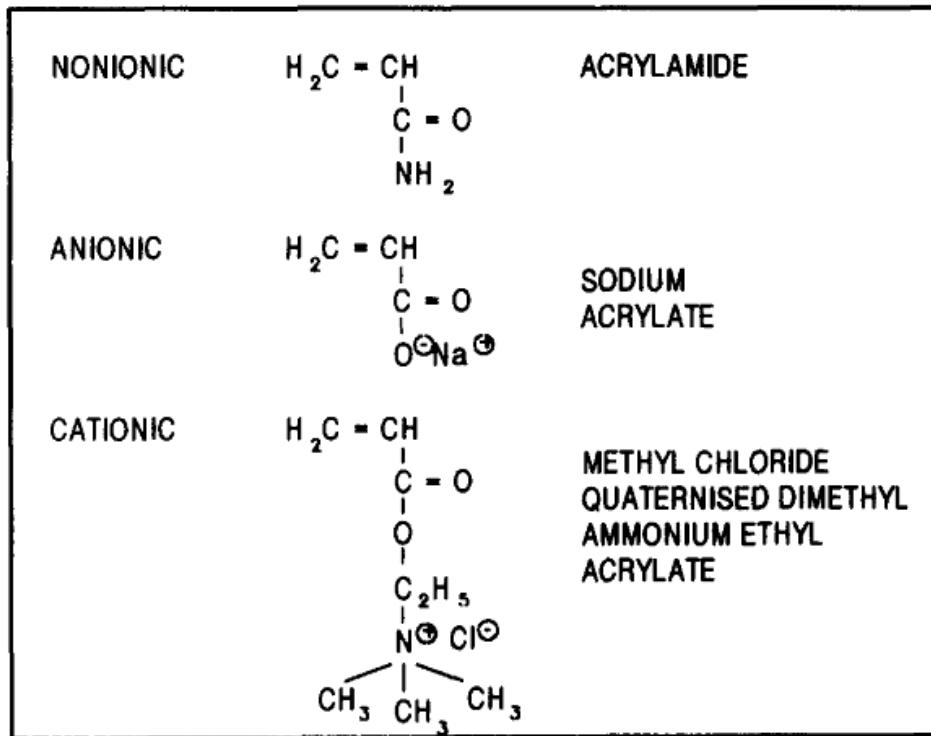


Figure 2.4 Examples of typical acrylamide based monomers (Moody, 1992)

#### 2.4.2 Previous Research of PAM as Depressant in Flotation

PAM has been applied to mineral processing industry for decades, but mainly limited to be the flocculants (Moody, 1992). However, there are still a few attempts in laboratory to use PAM and its derivatives as depressants for minerals separation.

Moudgil (1983) showed that non-ionic PAM depressed coal flotation. The depressive effect was attributed to the adsorption of the hydrophilic polymer



molecules on the coal particles which render the surface polar in nature.

Zhang et al. (2004) tested the depressive performance of hydroxamic PAM in the flotation of calcite, diasporite and pyrite. It was found that hydroxamic PAM showed intensive depression on pyrite. Mechanism study revealed that strong chemical interactions exist between hydroxamic PAM and pyrite surface.

Liu et al. (2007) studied the role of cationic PAM in the reverse flotation of diasporic bauxite. The reverse flotation separation of kaolinite and diasporite was achieved at pH 5.5–8.5 by using dodecylamine as a collector and cationic PAM as a depressant. Cationic PAM adsorbed on diasporite by hydrogen bond and electrostatic effect, prevented the majority of dodecylamine cationic species from adsorbing on the diasporite surface, and thus, depressed diasporite flotation.

Boulton et al. (2001) used low molecular weight PAM polymers to separate copper-activated sphalerite from pyrite in the presence of isobutyl xanthate (IBX). They grafted carboxyl, sulfonate, hydroxyl or thiourea functional groups to PAM to get PAMs with different characteristics. It was found that all the PAMs depressed pyrite with no or little depression of sphalerite. Besides, hydroxyl PAM showed the best depression while carboxyl PAM had the best selectivity.

A recent study by using xanthation modified polyacrylamide (PAM-X) and PAM as depressants on galena and sphalerite flotation was carried out (Wang et al., 2012). PAM-X was synthesized by grafting xanthate groups onto high molecular weight PAM. In single mineral flotation with PAM-X as a depressant and potassium ethyl xanthate as a collector, it was found that galena was completely depressed while copper activated sphalerite was still floatable at pH 11. When using PAM as a depressant, copper activated sphalerite was depressed while galena could be floated at pH 9 and pH 10.

#### *2.4.3 Adsorption Mechanism of PAM on Mineral Surface*

Linke and Booth (1960) proposed three possible mechanisms through which PAM may attach to mineral surface:

- 1) Hydrogen bonding: between the hydrogen of amide group and oxygen on the mineral surface
- 2) Specific, electrostatic site-bonding: between the carboxylate group in anionic PAM and metal ions in mineral lattice.
- 3) Nonspecific, double layer interaction: the electrostatic interaction due to dissimilar charges on the polymer and mineral surface.

Griot and Kitchener (1965) studied the adsorption of PAM onto silica by infrared

spectroscopic techniques. Peaks corresponding to hydrogen bonded hydroxyl groups and free hydroxyl groups were observed. The disappearance of peaks of free hydroxyl groups provided the evidence that hydrogen bonding formed between PAM and surface silanol groups.

Michaels and Morelos (1955) concluded that PAM adsorbed on kaolinite through hydrogen bonding between un-ionized carboxyl or amide groups on the polymer and oxygen at the mineral surface. At high pH where polymer adsorption by kaolinite did not occur, anionic polyelectrolytes caused flocculation through a reduction of the zeta potentials of the clays.

Read (1971) proposed that the adsorption of anionic PAM on hematite could involve carboxylate groups in the PAM and iron-hydroxyl complexes on the hematite.

Pradip and Fuerstenau (1980) investigated the adsorption of PAM as flocculants on apatite. They stated that the adsorption was mainly through hydrogen bonding between hydroxyl groups on apatite surface and amide group of PAM molecules, and also electrostatic forces.

At this point, there are few literature reports to reveal the adsorption mechanism of PAM on galena and chalcopyrite surface. However, some researchers have studied the adsorption mechanism between sulfide minerals and other polymers, which could be good references for the present study.

Liu and Laskowski (1989a; 1989b) studied dextrin adsorption on chalcopyrite and galena. They found that dextrin adsorbed on the sulfide surface through interactions with the surface metal hydroxide species. Dextrin-lead complex would be formed as a result of the interaction of dextrin with lead hydroxide. Such complexes were also found to form in ferric-dextrin and cupric-dextrin system.

Gong et al. (2010) studied the role of high molecular weight polyethylene oxide in reducing quartz gangue entrainment in chalcopyrite flotation. It was found that polyethylene oxide adsorbed on both quartz and chalcopyrite minerals mainly through hydrogen bonds, which were formed between the “free” ether oxygen of polyethylene oxide and “free” hydroxyl groups on mineral surfaces.

Huang et al. (2012b) investigated the adsorption of chitosan on chalcopyrite and galena from aqueous suspensions. They proposed that a chemical adsorption was formed between chitosan and chalcopyrite through the deacetylated unit (amine)

and the hydroxyl groups on chitosan. While chitosan-galena interaction was possibly due to weaker hydrophobic association through acetyl (amide) units of chitosan, which are present in chitosan as a result of incomplete deacetylation.

Wang et al. (2012) studied the adsorption mechanism of xanthation modified polyacrylamide (PAM-X) on galena and sphalerite by ATR-FTIR and XPS. The results indicated that the major interaction force between PAM-X and galena was sulfur chemical bond, while the only interaction force between PAM-X and sphalerite may be electrostatic force. It also appeared that the interaction between PAM and galena was hydrogen bond, while the interaction between PAM and sphalerite was electrostatic attraction caused by the protonation of hydrogen.

## **2.5 Surface Contamination by Metal Ions and EDTA Extraction**

When two or more minerals are in contact or mixed in a suspension, the released metal ions may remain on the originating mineral or transfer to the other mineral, resulting in variation of surface properties, and consequently, mineral floatability (Sui et al., 1995). For example, copper or lead ions can adsorb on sphalerite surface to make it floatable in the presence of xanthate collectors. Such a phenomenon is called copper or lead activation of sphalerite (Laskowski et al., 1997). Other observations of the effects on flotation attributed to metal ions have

been reported for copper ions on galena (Guy and Trahar, 1984), copper ions on pyrite (Chandra and Gerson, 2009), lead ions on quartz (Fuerstenau et al., 1965). However, some of these metal ion transfers are unwanted as they will cause surface contamination which adversely affect flotation. In practice, the unwanted metal ions can be removed by complexation reagents.

Ethylenediaminetetraacetic acid (EDTA) is a polyamino carboxylic acid and a colorless, water-soluble solid. EDTA is a well-known chelating agent for many metals, forming soluble EDTA-metal complex (Senior and Trahar, 1991). This is called EDTA extraction, which has been used to promote mineral flotation by removing unwanted metal ions from mineral surface (Guy and Trahar, 1984; Wang and Forssberg, 1990). It is also utilized as the means to determine the mineral surface metal ion concentration (Sui, et al., 1995). Besides the application in mineral processing, EDTA extraction is also used to remove heavy metal contamination from soil (Hong et al., 1999).

### **3. RESEARCH OBJECTIVES**

According to the literature review in Chapter 2, in the Cu-Pb differential flotation, non-toxic organic depressants need to be developed to substitute the traditional inorganic depressants such as cyanide and dichromate. PAM, as a widely used flocculant in mineral processing, has not been examined as a selective depressant in Cu-Pb differential flotation. Meanwhile, the limited number of research by using PAM as a depressant so far were all focused on low molecular weights. This means that PAM has not ever been tested as both a depressant and a flocculant in mineral flotation. The objective of this project is to focus on the selective depressive effect of PAM, to study:

- 1) if PAM has selective depressive effect on galena and chalcopyrite in single mineral flotation tests;
- 2) the adsorption mechanism of PAM on galena and chalcopyrite;
- 3) if PAM can separate galena and chalcopyrite from their mixtures.

## **4. EXPERIMENTAL MATERIALS AND METHODS**

### **4.1 Materials and Reagents**

Natural galena, chalcopyrite, sphalerite and pyrite minerals were purchased from Ward's Scientific Establishments, Ontario, Canada. The lumps of each mineral were separately crushed (Retsch jaw crusher, USA) and hand-picked to obtain high purity samples, and then further crushed and pulverized with a Pulverisette 2 mechanized agate mortar/pestle grinder (Fritsch, Germany). The -75+38  $\mu\text{m}$  size fractions were screened out for use in the flotation test. The -38  $\mu\text{m}$  size fractions were utilized for surface analysis. In order to minimize oxidation, all mineral samples were sealed in plastic bottles and stored in a freezer at -10  $^{\circ}\text{C}$ .

X-ray diffraction measurements on the chalcopyrite and galena samples showed that there were minor amounts of quartz in chalcopyrite and no impurities in galena. Chemical analysis of the samples showed that the chalcopyrite sample contained 29.26% Cu, representing a purity of 84.5% chalcopyrite, and that galena contained 84.00% Pb, indicating a high purity of 97.0% galena.

Non-ionic PAM was of analytical grade with high purity (99.999%) and a molecular weight of 5,000,000–6,000,000 purchased from ACROS Canada Inc. Hydrochloric acid and sodium hydroxide (Fisher Scientific Canada) were used to



adjust pH. Potassium ethyl xanthate (KEX) was obtained from Prospec Chemicals Ltd, Canada, and used as a collector in the flotation tests. It was purified by washing with ethyl ether anhydrous and acetone (Fisher Scientific Canada) following the protocol of Foster (Foster, 1928) before use.  $\text{CuSO}_4 \cdot 5\text{H}_2\text{O}$  (Fisher Scientific Canada) was used as the source of  $\text{Cu}^{2+}$  ion in the solution to activate sphalerite. Distilled water was used throughout the tests.

## **4.2 Experimental Procedure**

### *4.2.1 Froth flotation*

The froth flotation tests were conducted in a small-scale flotation tube (Figure 4.1). The bottom of this tube was a sintered glass frit with a pore size of 1.6  $\mu\text{m}$  on which a magnetic stirring bar could be used to agitate the flotation pulp. The top of the flotation tube was modeled after Siwek et al. (1981). The throat that connects flotation tube and the collection bulb was narrow that only one gas bubble could pass through it at one time when no frother was used, thus minimizing mechanical entrainment.



Figure 4.1 Small scale-flotation tube

In single mineral flotation test, 1.5 g single mineral sample with particle sizes of -75+38  $\mu\text{m}$  was first washed by 0.1% HCl and then by distilled water. The washed sample was mixed with 150 mL distilled water in a 250 mL beaker. The pH of the suspension was adjusted to appropriate values by NaOH or HCl. This was followed by the addition of stock PAM solution (with a concentration of 1 g/L) and stock potassium ethyl xanthate solution (1.2 g/L), with 3 minutes stirring after adding each reagent, respectively. The conditioned slurry was transferred to the flotation tube and floated for 5 min using high purity nitrogen gas. In sphalerite flotation,  $10^{-4}$  M  $\text{CuSO}_4$  solution was used as an activator prior to the addition of

the polymer depressant. The mineral recovery was calculated from the dry weights of the flotation concentrates and tails.

In mineral mixture flotation, 1 g each of galena and chalcopyrite were mixed as flotation feed sample, and the procedure was the same as above. In mineral mixture flotation, EDTA was used in selected tests. When it was used, the stock EDTA solution (with a concentration of 1 g/L) was added before the addition of PAM solution. After flotation, both the froth product and tailings were collected, dried, weighed, and assayed for Cu and Pb contents. This was done by dissolving the dried samples with aqua regia and analyzing the solutions using a Varian SpectrAA-220FS (Varian, USA) atomic absorption spectrometer (AAS).

#### *4.2.2 Contact Angle Measurements*

The contact angle measurements were conducted using a Krüss drop shape analysis system (DSA 10-MK2, Germany), as shown in Figure 4.2. A sessile drop method was utilized to determine the contact angle of water on the surface of a 10 mm diameter pressed pellet of powdered mineral samples. The samples ( $\sim 38\mu\text{m}$ ) were prepared by following the same procedure in single mineral flotation. The pellet was prepared from  $\sim 0.3$  g of fine mineral under a pressure of 5000 psi (340 atm) (ICL International Crystal Laboratories, USA) for 3 min. A drop of distilled

water was placed on the surface of the pressed pellet and a set of microscopic images of the drop and the pellet were taken immediately. Then one image with the best stable view was chosen to determine the contact angle by fitting a tangent to the shape of the sessile drop on the microscopic image.

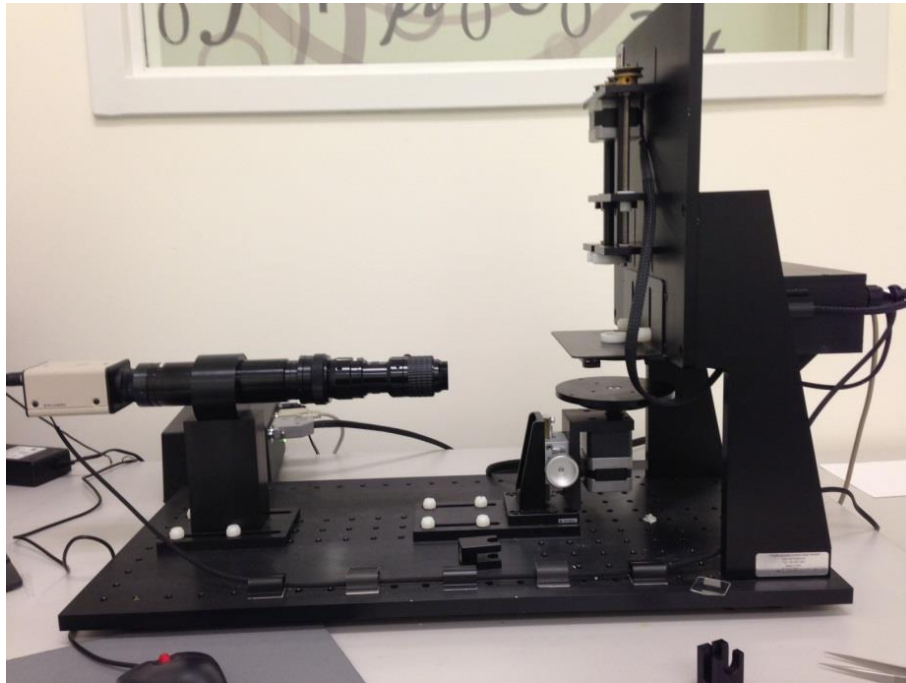


Figure 4.2 Krüss DSA 10 Mk2 drop shape contact angle measuring instrument.

#### *4.2.3 Zeta Potential Measurements*

Zeta potential measurements were conducted using a ZetaPALS Zeta Potential Analyzer manufactured by Brookhaven Instruments, as shown in Figure 4.3. The zeta potentials were calculated from measured electrophoretic mobility by the

Smoluchowski model. Each reported zeta potential value is the mean of 10 runs, with 20 measurement cycles per run. To minimize error, the highest and lowest runs were not counted in the calculation of mean zeta potential. The procedure of sample preparation for zeta potential was as follows:

1. Prepare the stock mineral suspension by adding 0.1 g of -38  $\mu\text{m}$  mineral to 100 mL of  $10^{-2}$  mol/L KCl solution in a 100 mL volumetric flask. Allow the suspension to stand for 24 hours.
2. Vigorously agitate the mineral suspension and withdraw 10 mL into a 250 mL beaker. Then add 90 mL  $10^{-2}$  mol/L KCl solution to the beaker, making a total suspension volume of 100 mL.
3. Add 0.5 mg/L PAM to the suspension if necessary
4. Adjust pH and condition the suspension for 20 minutes at each value of pH. Separate suspensions were used for acid pH range measurements and alkaline pH range measurement, using natural pH as the starting point. To avoid dilution of KCl concentration, KOH and HCl solutions prepared by  $10^{-2}$  mol/L KCl solution were used to adjust pH.
5. After conditioning, transfer  $\sim 2$  mL of conditioned solution to a disposable plastic sample cuvette for measurement.

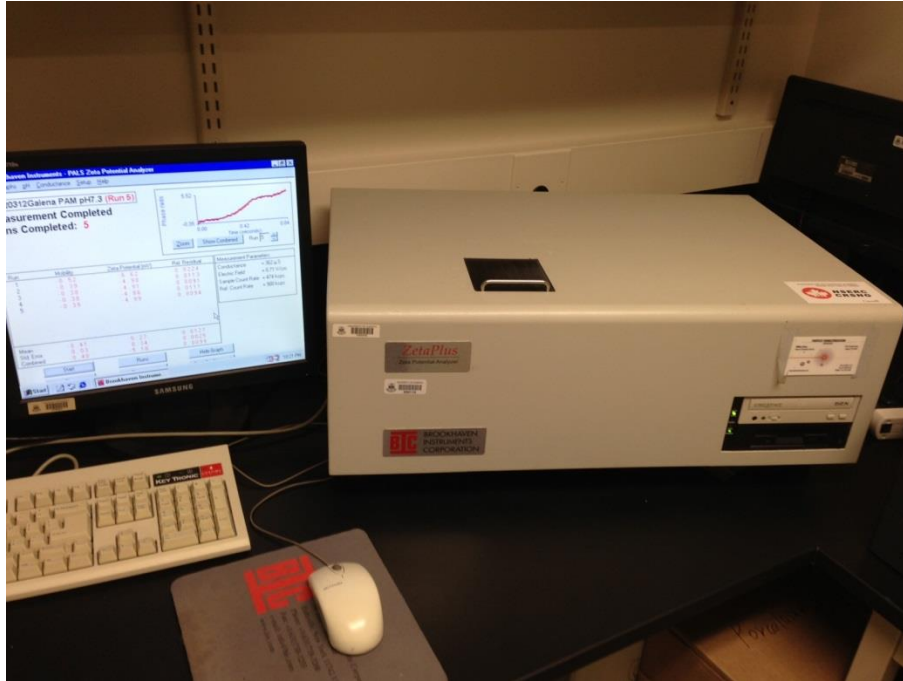


Figure 4.3 ZetaPALS Zeta Potential Analyzer.

#### *4.2.4 X-Ray Element Mapping Measurements*

X-ray element mapping measurements were conducted using a Hitachi S-2700 Scanning Electron Microscope (SEM) equipped with a PGT (Princeton Gamma-Tech) IMIX digital imaging system and a PGT PRISM IG (Intrinsic Germanium) detector for Energy Dispersive X-Ray Analysis (EDX). The Backscattered Electron Detector is GW Electronics System 47 four quadrant solid state backscattered electron detector. The standard operating conditions for X-ray element mapping have been at 20 kV accelerating voltage, 17 mm working distance, and a beam current of between 1-1.5 nA. The  $-75+38 \mu\text{m}$  mineral

particles were used for the measurements and the samples were prepared following the same procedures as in mineral mixture flotation.

#### *4.2.5 ToF-SIMS Measurements*

Time of flight secondary ion mass spectrometric (ToF-SIMS) measurements were conducted using a ToF-SIMS IV - 100 spectrometer (ION-TOF GmbH), as shown in Figure 4.4, using 25 keV Bi<sup>+</sup> primary ions. The area of each sample for spectra acquisition was 146.5  $\mu\text{m}$   $\times$  146.5  $\mu\text{m}$ . The positive ion spectra, as a function of mass, were calibrated using the H<sup>+</sup>, CH<sub>3</sub><sup>+</sup> and Na<sup>+</sup> peaks. Images were generated by mapping the mass-selected ion intensity in a burst alignment mode with 128  $\times$  128 pixels per image. The spectra of four samples were recorded, including two pure chitosan samples and the two mineral samples. The mineral samples were prepared by mixing chalcopyrite and galena at a weight ratio of 1:1 in 100 mL distilled water at pH 10, and adding 8 mg/L of PAM, 20 mg/L EDTA if used. The suspension was conditioned in a shaking incubator for 30 min equilibrated at 25  $^{\circ}\text{C}$ , and the minerals were filtered, washed with distilled water through the filtration funnel and dried in a desiccator under vacuum before analysis. To minimize oxidation, the ToF-SIMS analysis was conducted within 12 hours after mineral sample preparation.

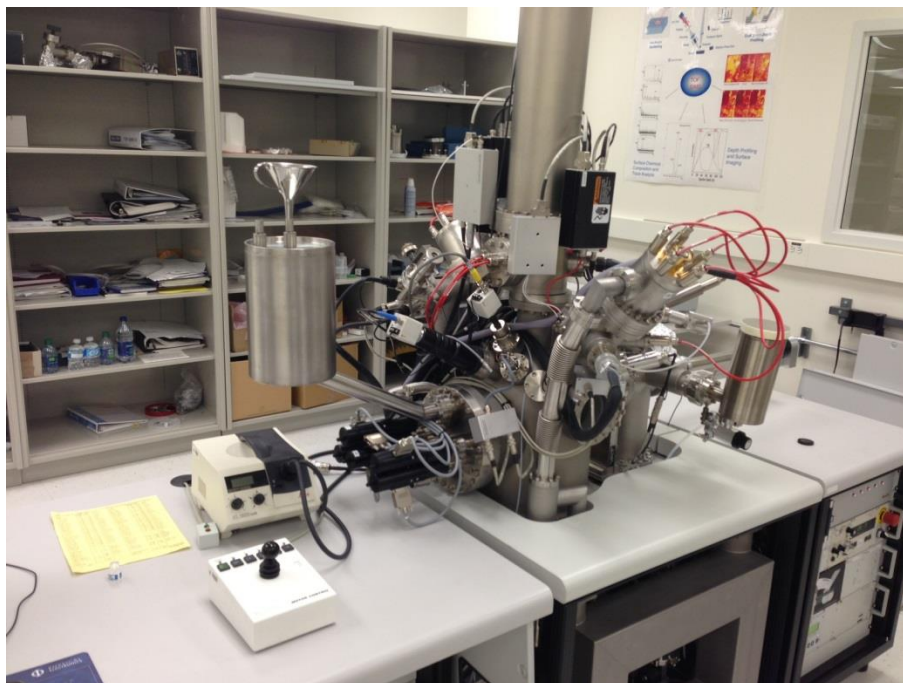


Figure 4.4 ToF-SIMS IV - 100 spectrometer (ION-TOF GmbH)

#### 4.2.6 XPS Measurements

X-ray photoelectron spectroscopy (XPS) survey scan and high-resolution spectra were acquired on an AXIS 165 X-ray photoelectron spectrometer (Kratos Analytical), as shown in Figure 4.5. Monochromatic Al K $\alpha$  source ( $h\nu = 1486.6$  eV) was used at a power of 210W for all data acquisition. The vacuum pressure inside the analytical chamber was lower than  $3 \times 10^{-8}$  Pa. The analyzed area on the sample surface was  $400 \mu\text{m} \times 700 \mu\text{m}$ . To prepare the mineral sample for the XPS analysis, 1 g chalcopyrite or galena was mixed with 8 mg/L of PAM in 100 mL distilled water at pH 10. The suspension was conditioned in the incubator for 30



min, and the mineral solids were filtered, washed with distilled water through the filter funnel and dried in a desiccator in vacuum before XPS analysis. To minimize oxidation, the analysis was carried out within 12 h after sample preparation. The survey scans were collected for binding energy range from 1100 eV to 0 eV with analyzer pass energy of 160 eV and a step of 0.4 eV. To collect the high-resolution spectra, the pass-energy was set at 20 eV with a step of 0.1 eV. No charge neutralization was required through the spectra collection. XPS sampling depth for photoelectrons was 3 – 10 nm, which was more than enough to provide information of the mineral surfaces in this work. CasaXPS version 2.3.15 instrument software was used to process the XPS data after spectra collection. The Shirley-type background subtraction was chosen to optimize the peak height through the high-resolution spectra analysis. And then, according to previously published data, the processed spectra were calibrated, resolved and refined into individual Gaussian – Lorentzian peaks and imported into a graphic software, Origin.

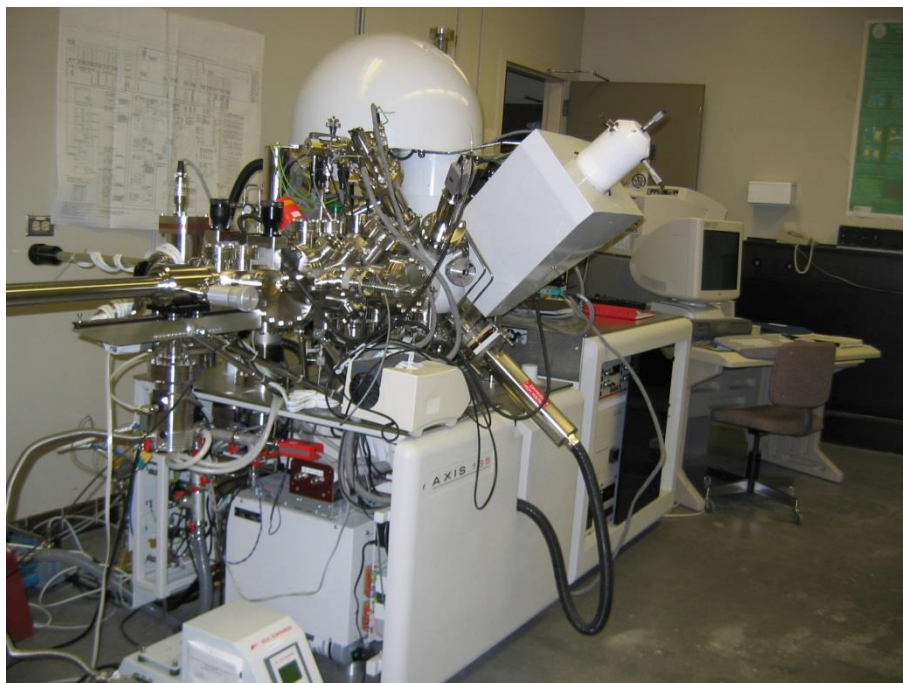


Figure 4.5 Axis 165 X-ray Photoelectron Spectrometer (Kratos Analytical).

## 5. RESULTS AND DISCUSSION

### 5.1 Single Sulfide Mineral Flotation

Small scaled single mineral flotation tests were conducted on several common sulfide minerals including galena, chalcopyrite, pyrite and sphalerite. The flotation recovery of these sulfide minerals without adding any depressant is shown in Figure 5.1 as a baseline. It can be seen that galena, chalcopyrite and sphalerite (copper activation) are floatable in the tested pH range from 9 to 11.

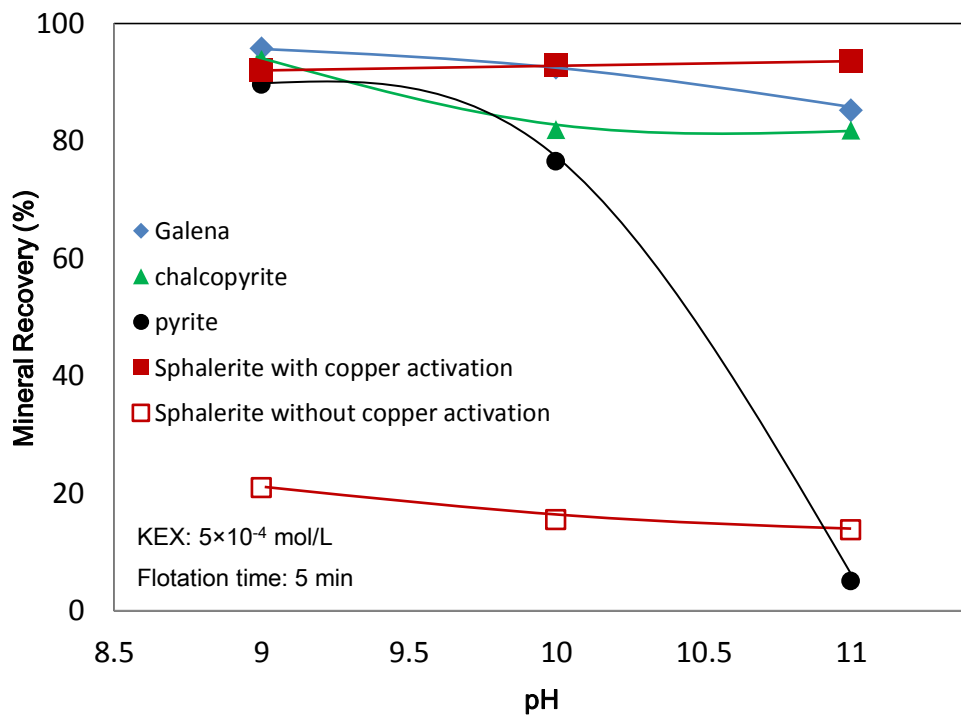


Figure 5.1 Recovery of single sulfide mineral flotation as a function of pH in the absence of PAM as depressant. (KEX:  $5 \times 10^{-4}$  mol/L; Condition time: 3 min; Flotation time: 5 min).

The floatability of sphalerite without activation is as low as 20% in this pH range.

For pyrite, as it is floatable at pH 9, its flotation recovery drops sharply at pH > 10.

The results agree with previous literature (King, 1982).

This single mineral flotation results indicate that except for pyrite at pH > 11, there is no separation possibility between these sulfide minerals in the absence of any depressant.

Figure 5.2 shows the flotation behavior of the sulfide minerals in the presence of 8 mol/L PAM (added before KEX). Compared with Figure 5.1, the difference in the floatabilities for each sulfide mineral can be seen in the presence and absence of PAM. For galena, the depressive effect of PAM is minor from pH 9 to pH 10. With increasing pH from 10 to 11, galena recovery drops to around 50%. For sphalerite with copper activation, PAM can depress its flotation recovery. While it is highly floatable without any depressant in the pH range from 9 to 11, its recoveries drop to 40% ~ 20% in the presence of PAM. For chalcopyrite, pyrite and sphalerite without activation, the depressive effect of PAM are more remarkable. These minerals cannot float in the pH range from 9 to 11. The result indicates that, except galena, all other sulfide minerals are depressed by the addition of PAM in medium alkaline solution. This means PAM could be used as a depressant to separate galena from other sulfide minerals. In this project, the

study was focused on the separation of galena and chalcopyrite. The adsorption mechanism of PAM on galena and chalcopyrite were studied.

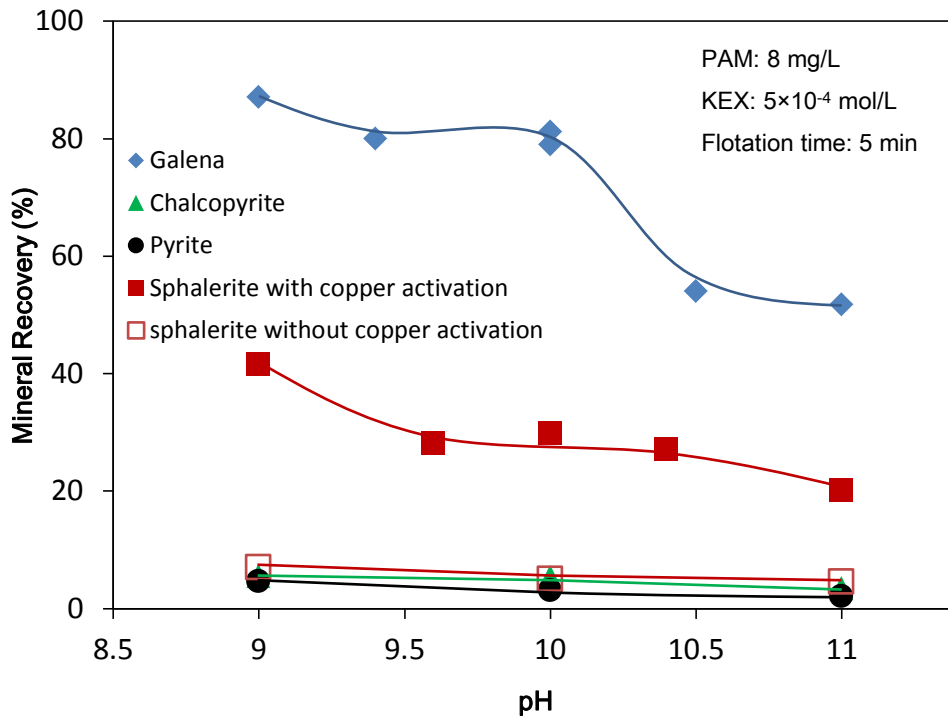


Figure 5.2 Recovery of single sulfide mineral flotation as a function of pH in the presence of PAM as a depressant. (PAM: 8 mg/L; KEX: 5×10<sup>-4</sup> mol/L; Condition time: 3 min; Flotation time: 5 min).

## **5.2 Adsorption Mechanism of PAM on Galena and Chalcopyrite**

### *5.2.1 Zeta Potential Measurement*

Zeta potential measurements were conducted for galena and chalcopyrite, before and after the addition of PAM. The results are shown in Figure 5.3. The zeta potential of galena is always negative and decreases with increasing pH. The i.e.p. value (isoelectric point) is around pH 3 according to this trend. Chalcopyrite has a positive zeta potential in strong acidic solutions with an i.e.p. at about 3.5. At pH higher than the i.e.p., the zeta potential becomes negative and also decreases with increasing pH. The tested zeta potential values of galena and chalcopyrite are consistent with the reported values in the literature (Kelebek and Smith, 1989).

After the addition of 0.5 mol/L PAM, the magnitude of the zeta potential for both galena and chalcopyrite decreased, but the i.e.p. and the signs did not change. This indicates that PAM adsorbed on the surfaces of both minerals. As the PAM used was non-ionic, its adsorption could stretch the shear plane of the electrical double layer on mineral surface further away from the surface, lowering the magnitude of the zeta potential. However, since PAM could not selectively change the electrokinetic properties of galena and chalcopyrite, the electrostatic interaction was ruled out as the possible interaction mechanism responsible for the observed selectivity of PAM in single mineral flotation of galena and

chalcopyrite.

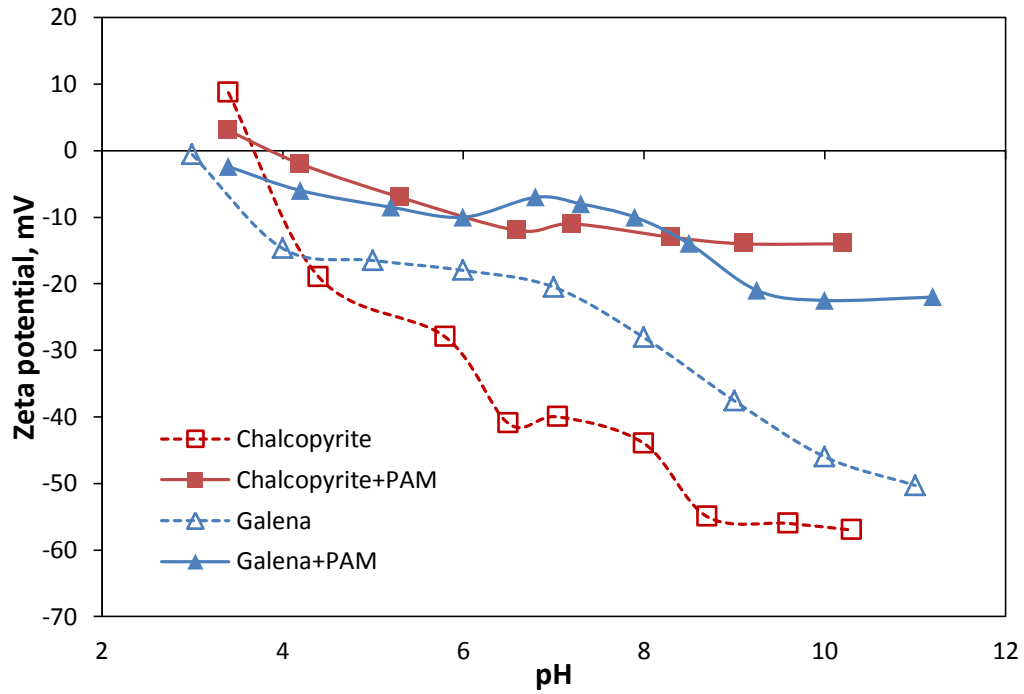


Figure 5.3 Zeta potential versus pH for galena and chalcopyrite conditioned in 0.01 mol/L KCl solution, with and without PAM.

### 5.2.2 Contact Angle Measurement

The hydrophobicity of galena and chalcopyrite before and after PAM and collector adsorption was characterized by contact angle measurements. The results are shown in Figure 5.4.

The contact angle of galena and chalcopyrite without any reagent were measured to be  $78 \pm 2.5^\circ$  and  $76 \pm 2.5^\circ$ , respectively, as shown in Figure 5.4 (a), (d). This indicates that both galena and chalcopyrite at pH 10 have good hydrophobicity in the absence of any depressant. After PAM adsorption, the contact angles of galena and chalcopyrite drop to  $33 \pm 1.7^\circ$  and  $36 \pm 1.8^\circ$ , respectively, as shown in Figure 5.4 (b), (e). This means PAM could adsorb on both galena and chalcopyrite to decrease their surface hydrophobicity. For the last two samples, KEX were added to solution after PAM adsorption, which is exactly the same procedure as in the flotation tests. Figure 5.4 (c) shows that the contact angle of galena after KEX addition increased back to  $70 \pm 2.4^\circ$ , which is similar to the one without PAM and KEX addition shown in Figure 5.4 (a). However, the contact angle of chalcopyrite after KEX addition is  $52 \pm 2.1^\circ$  as shown in Figure 5.4 (f), which shows that chalcopyrite still has a relatively lower hydrophobicity than galena after the same sequential treatment by PAM and xanthate.



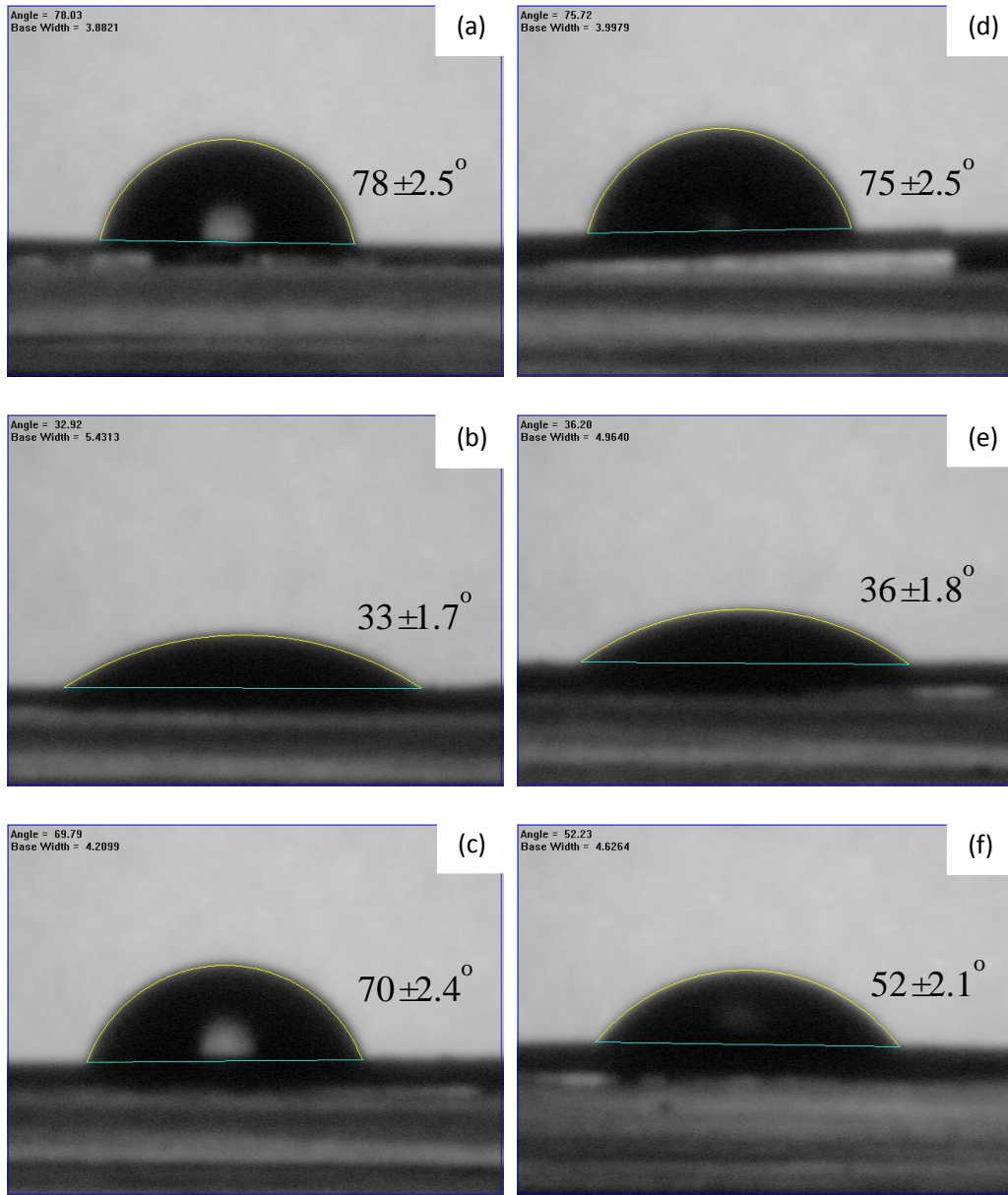


Figure 5.4 The contact angle images of a water sessile drop on the pressed pellet of (a) galena, (b) galena after PAM adsorption, (c) galena after PAM and KEX adsorption, (d) chalcopyrite, (e) chalcopyrite after PAM adsorption, (f) chalcopyrite after PAM and KEX adsorption. (pH = 10; PAM: 8 mg/L; KEX:  $5 \times 10^{-4}$  mol/L; pellet press pressure: 5000 psi.)

The contact angles results show how PAM and KEX can change the surface hydrophobicity of galena and chalcopyrite. The results agree with the single mineral flotation results, that PAM can depress chalcopyrite but not galena. While PAM can adsorb on both galena and chalcopyrite, the affinity between PAM and chalcopyrite should be stronger than that with galena. Thus KEX can almost completely break up the bond between PAM and galena to make galena hydrophobic again, but not for chalcopyrite. It is the combined use of PAM and KEX that caused the selective depressive effect between galena and chalcopyrite.

### *5.2.3 XPS Measurement*

X-ray photoelectron spectroscopic (XPS) technique was utilized to investigate the adsorption mechanism of PAM on galena and chalcopyrite. The XPS survey scan and the narrow scan of N 1s spectra were first performed on PAM. Survey scan of PAM is shown in Figure 5.5 (a). Three peaks are identified near 290 eV, 400 eV and 530 eV which correspond to C 1s, N 1s and O 1s, respectively (Wagner, 2003). Figure 5.5 (b) shows the N 1s narrow scan of PAM. The measured peak was deconvoluted into two peaks. The peak at 399.7 eV originates from -NH-C=O (amide) bond (Hantsche, 1993; Uchida et al., 1990; Wang, et al., 2012), which was used as an internal standard to correct the shift caused by charging effect. The other peak at 400.5 eV is assigned to amino groups in ammonium form ( $\text{NH}_3^+$ )

(Lindberg et al., 1983). Both forms,  $\text{NH}_2$  and  $\text{NH}_3^+$ , are likely to be present in PAM. In acrylamide molecule, the carbonyl and amide form a conjugation structure, which enhances the polarity of N-H and makes it easily protonated to form  $\text{NH}_3^+$ .

The relative intensity (RI) of amide and ammonium are 90.9% and 9.1%, respectively, based on the integrated areas of the two peaks.

The survey scans and narrow scans of N 1s were then performed on chalcopyrite and galena before PAM and KEX treatment. The two peaks originating from Cu  $(2p)_{3/2}$  at 932.0 eV on chalcopyrite spectrum (not shown) and Pb  $(4f)_{7/2}$  at 137.5 eV on galena spectrum (not shown) were used to calibrate the entire XPS spectra of chalcopyrite and galena, respectively. The results of N 1s narrow scans are shown in Figure 5.6 (a), (b). As can be seen, no peaks corresponding to N species were observed for either galena or chalcopyrite on their high resolution spectra.

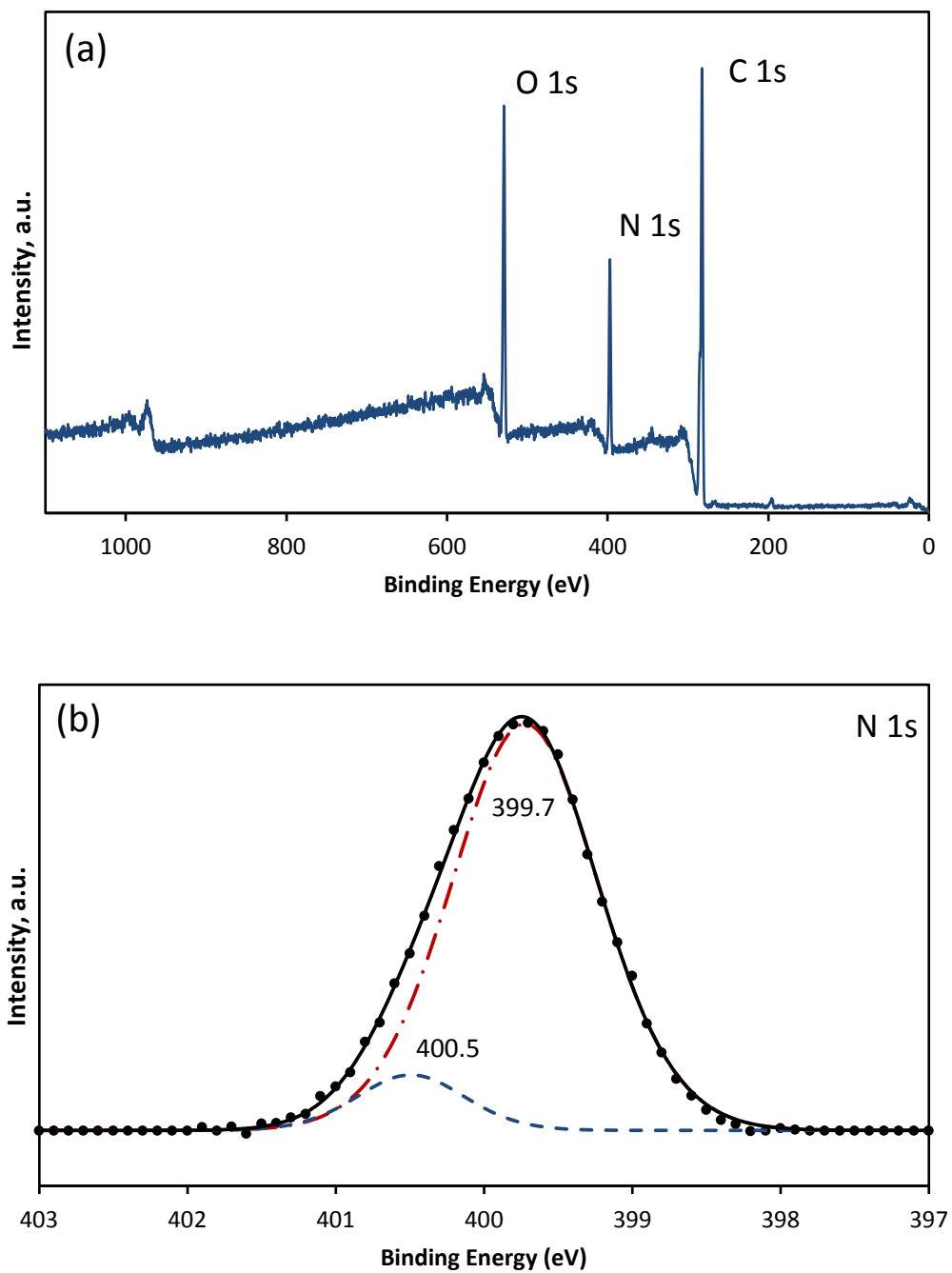


Figure 5.5 XPS spectra of PAM by (a) survey scan, (b) N 1s narrow scan.

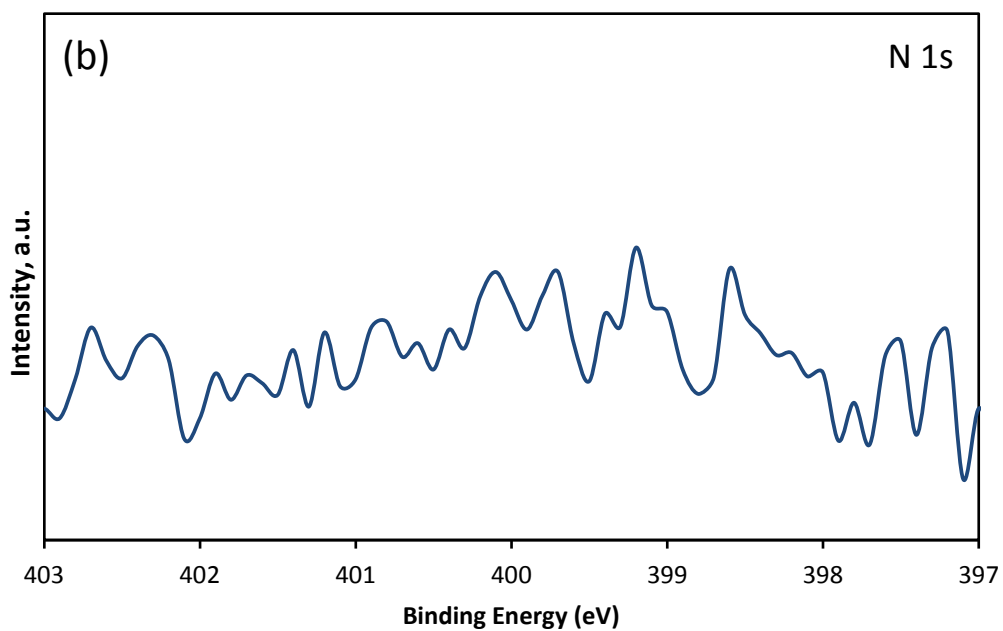
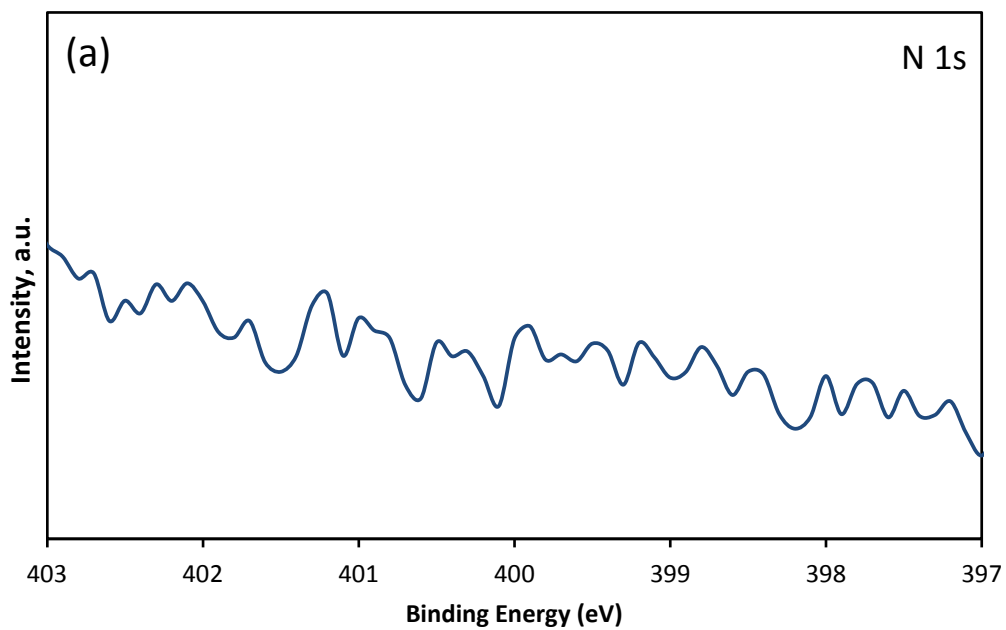
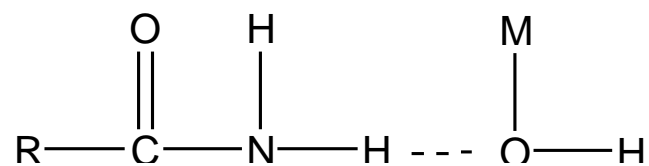


Figure 5.6 XPS spectra of N 1s narrow scan for (a) galena, (b) chalcopyrite.

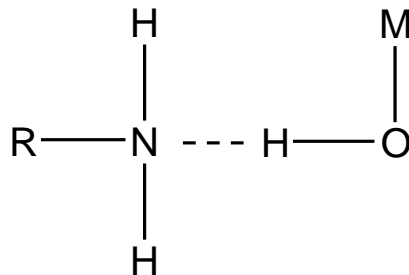
For both galena and chalcopyrite, the N 1s peaks were observed on their XPS survey scans (not shown) after PAM adsorption, indicating the presence of PAM on their surfaces. In order to identify the species of nitrogen on the mineral surfaces, narrow scans of N 1s were carried out. The N 1s spectrum on galena after PAM adsorption is shown in Figure 5.7 (a). As can be seen, only one peak corresponding to amide was observed while no peak corresponding to ammonium was detected, indicating that PAM adsorbed on galena only through the amide group. The binding energy of amide shifted to 399.6 eV from 399.7 eV in PAM. At pH 10, galena surface are mainly covered by lead hydroxide (King, 1982). The most likely interaction between PAM and galena is through hydrogen bonding. The hydrogen bonding may form between hydrogen atom of amide in PAM and oxygen atom of hydroxyl group in lead hydroxide:



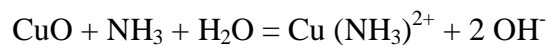
The slight shift in binding energy was probably caused by the formation of hydrogen bonding. This is consistent with the widely accepted view that PAM can adsorb on mineral surface (silica, kaolinite, apatite etc.) through hydrogen bonding (Griot and Kitchener, 1965; Michaels and Morelos, 1955; Pradip and Fuerstenau, 1980). In a recent study, Wang, et al. (2012) investigated the adsorption of PAM on galena by using attenuated total reflectance Fourier

transform infrared spectroscopy (ATR-FTIR). They observed stronger intensity of N-H deformation than C=O stretching, and the peak shift for N-H deformation, which also suggested that hydrogen bonding may have formed between amide group and galena.

Figure 5.7 (b) shows the N 1s spectrum of chalcopyrite after PAM treatment. The two peaks corresponding to amide and ammonium groups were both retained on spectrum, suggesting that the adsorption of PAM on chalcopyrite involves both amide and ammonium groups. Compared to pure PAM, the binding energy of amide shifted from 399.7 eV to 399.6 eV, while the binding energy of ammonium shifted from 400.5 eV to 400.4 eV. The relative intensity of amide group and ammonium group were 78.4% and 21.6%, respectively, while in PAM they were 90.0% and 9.1%. At pH 10, copper hydroxide and iron hydroxide are the major species on chalcopyrite surface. For amide group interaction, similar to PAM-galena, the hydrogen bonding may form between the hydrogen atom of the amide group in PAM and the oxygen atom of the hydroxyl group in copper hydroxide and iron hydroxide on mineral surface. For ammonium group interaction, since at pH 10 there are not a lot of protons  $H^+$  in the solution for amine groups  $NH_2$  to protonate, the ammonium group may first form by hydrogen bonding between the nitrogen atom of amine in PAM and hydrogen atom in the hydroxyl group in copper hydroxide or iron hydroxide:



Meanwhile, the formed ammonium group may further react with copper through a chemical complexation to form  $\text{NH}_3\text{-Cu}$  complex. This is consistent with the well-known process “ammonia leaching” in which ammonia  $\text{NH}_3$  is used to dissolve copper, nickel, cobalt, etc. (C.-Y. Lu and Graydon, 1955; Halpern, 1953; Meng and Kenneth, 1996). The reaction of ammonia with copper can be formulated as follow:



The shift in binding energy and the increased relative intensity for ammonium peak in N 1s spectra confirmed these interactions between ammonium and chalcopyrite surface. However, as ammonia leaching has been used to dissolve many metals, no records showed ammonia can react with lead. Morel (1983) listed the stability constants and complexing ligands of various metals including copper, nickel, cobalt, etc., but not for lead. In other words,  $\text{NH}_3\text{-Pb}$  complex probably does not exist. This agrees with the result in Figure 5.7 (a) that no ammonium can be detected on galena after PAM adsorption.



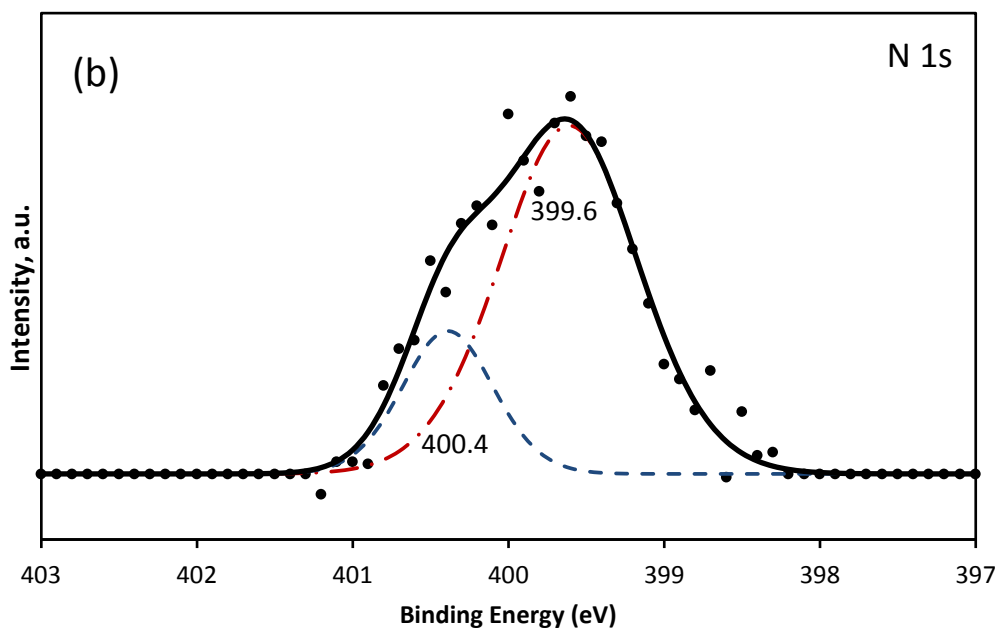
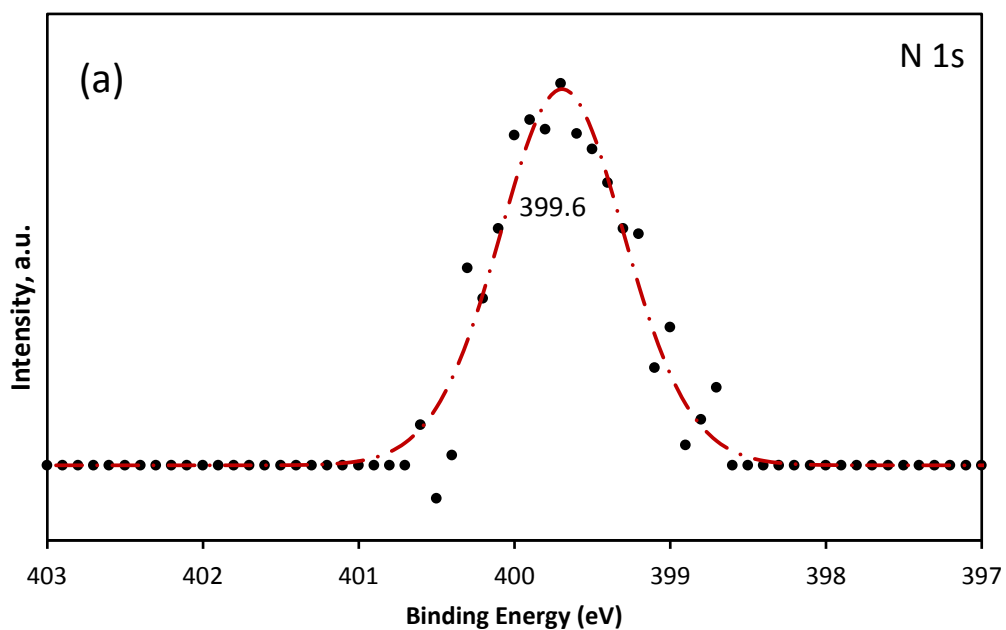


Figure 5.7 XPS spectra of N 1s narrow scan for (a) galena after PAM treatment, (b) chalcopyrite after PAM treatment.

The N 1s spectrum of galena after PAM and KEX adsorption is shown in Figure 5.8 (a). It can be seen that the peak for amide group disappeared after KEX adsorption, suggesting that PAM that adsorbed on galena surface have been removed by KEX. It has been widely accepted that xanthate adsorb on galena through a two-step adsorption process: the chemical reaction of xanthate ion and surface lead ion to form Pb-X complex, and the formation of multiple layers of lead xanthate by replacing oxidized products on the surface (King, 1982). At pH 10, galena surface are covered by lead hydroxides and metal-deficient sulfides. When PAM was first added, it attached to hydroxides through hydrogen bonding. Then when KEX was added, it chemically reacted with both lead hydroxides and metal-deficient sulfides to produce lead xanthate, dixanthogen and some other xanthate products. These precipitates would break up the previous formed hydrogen bonding between PAM and hydroxides. Gong (2011) found the similar phenomenon that potassium amyl xanthate (KAX) could destroy the hydrogen bonding between polyethylene oxide (PEO) and chalcopyrite.

Figure 5.8(b) shows the N 1s spectrum of chalcopyrite after PAM and KEX adsorption. After adding KEX, the two peaks at 399.6 eV and 400.4 eV can be observed, without too much binding energy shift compared with Figure 5.7 (b). This indicates that PAM still adsorbed on chalcopyrite surface after KEX addition. Compared to the relatively weak hydrogen bonding between PAM and galena, the

ammonium-copper chemical complex had a higher affinity that could not be destroyed by xanthate. The relative intensity of amide and ammonium were 72.1% and 27.9%, respectively, while before KEX addition they were 78.4% and 21.6%. The lower relative intensity of amide suggested that a small part of hydrogen bonds were replaced by xanthate such as the case of galena.

The positions of N 1s binding energy and relative intensity of all the peaks on galena and chalcopyrite after treatment with PAM or PAM and KEX are summarized in Table 5.1. The results of XPS measurements are consistent with those of contact angle measurements and single mineral flotation. They show that PAM would adsorb on galena and chalcopyrite through different mechanisms, chalcopyrite-PAM bonding is stronger than galena-PAM bonding. KEX can only break up the PAM adsorption on galena but not for chalcopyrite. As a result, in single mineral flotation by adding PAM and KEX, galena is floatable and chalcopyrite is depressed.

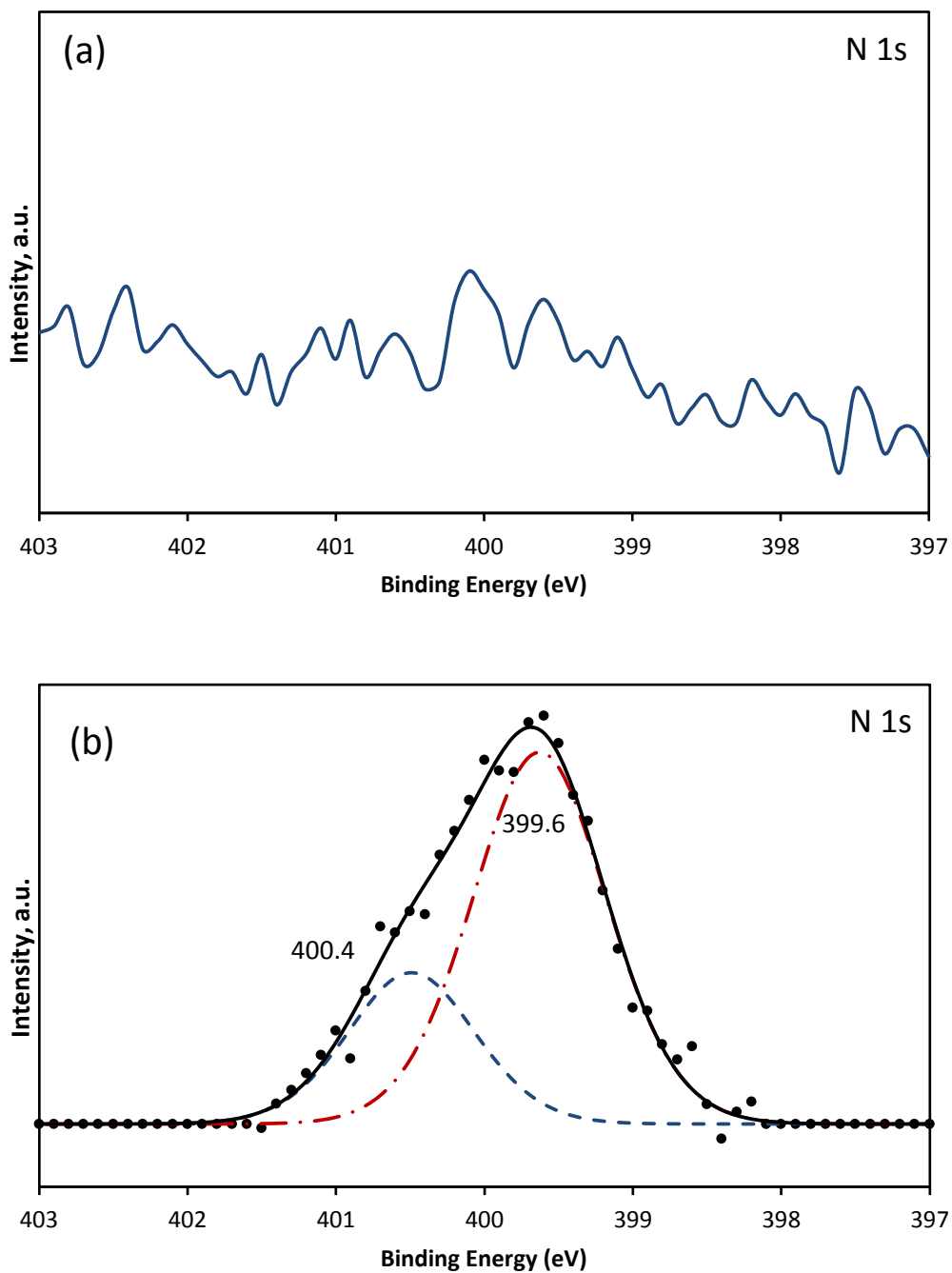


Figure 5.8 XPS spectra of N 1s narrow scan for (a) galena after PAM and KEX treatment, (b) chalcopyrite after PAM and KEX treatment.

Table 5.1 Binding energy and relative intensity of N 1s peaks of PAM, and galena and chalcopyrite with PAM or with PAM and KEX

Species	PAM			
	BE (eV)	RI (%)		
Amide (-NH-C=O)	399.7	90.9		
Ammonium (NH <sub>3</sub> <sup>+</sup> )	400.5	9.1		
	Chalcopyrite - PAM		Chalcopyrite - PAM - KEX	
	BE (eV)	RI (%)	BE (eV)	RI (%)
Amide (-NH-C=O)	399.6	78.7	399.6	72.1
Ammonium (NH <sub>3</sub> <sup>+</sup> )	400.4	21.6	400.4	27.9
	Galena - PAM		Galena - PAM- KEX	
	BE (eV)	RI (%)	BE (eV)	RI (%)
Amide (-NH-C=O)	399.6	100	N/A	N/A
Ammonium (NH <sub>3</sub> <sup>+</sup> )	N/A	N/A	N/A	N/A

## **5.3 Galena and Chalcopyrite Mixture Flotation**

### *5.3.1 Galena and Chalcopyrite Mixture Flotation without Surface Cleaning*

The galena and chalcopyrite mixture (weight ratio 1:1) flotation tests were conducted by varying the dosage of PAM at a constant pH of 10. The experiment procedure was the same as in single mineral flotation. As can be seen from the results shown in Figure 5.9, when no PAM was added, both galena and chalcopyrite are highly floatable with more than 90% recovery. This is similar with the result in single mineral flotation shown in Figure 5.1. However, both galena and chalcopyrite were depressed with increasing PAM dosage from 0.5 mg/L to 8 mg/L, while in single mineral flotation only chalcopyrite was depressed. Therefore, the separation window that was observed in single mineral flotation was absent in the mineral mixture tests.

To find out the possible reasons that affected the selectivity of PAM, it is important to note that the recoveries of galena at each tested PAM dosage were all close to that of chalcopyrite. In other words, galena behaved like chalcopyrite in the mineral mixture flotation. Thus, the most likely reason for the disappearance of selectivity of PAM in mixture flotation is that copper ions adsorb on galena surface prior to the PAM adsorption. This assumption is consistent with literature which reported that copper ions will transfer to galena surface in an aqueous

solution (Rao and Natarajan, 1990). If this is the case, PAM would adsorb on copper-contaminated galena surface, so that galena would behave like chalcopyrite. As a result, galena would be depressed as well as chalcopyrite.

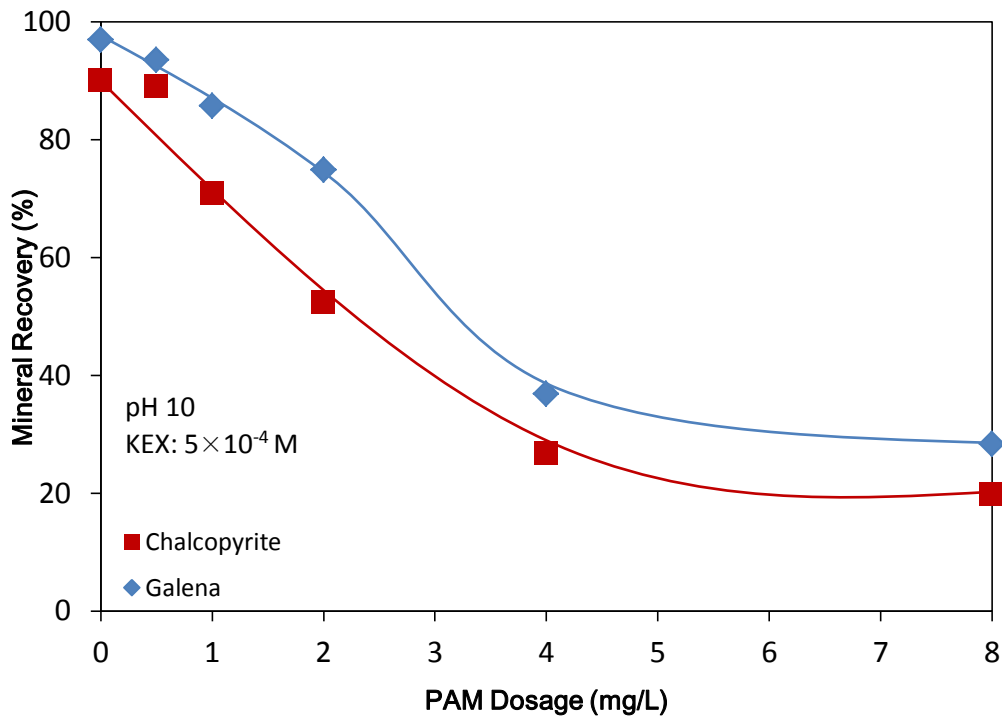


Figure 5.9 Recovery of the mixture of chalcopyrite and galena (weight ratio 1:1) flotation as a function of PAM dosage. (KEX:  $5 \times 10^{-4}$  mol/L; Condition time: 3 min; Flotation time: 5 min).

### *5.3.2 X-ray Element Mapping Measurements*

To prove the assumption that copper can contaminate galena surface when they are mixed in the slurry, the energy-dispersive X-ray (EDX) element mapping measurements were employed. The sample was prepared by following the same procedure in galena and chalcopyrite mixture flotation without adding PAM and KEX. Figure 5.10 (a) shows the back-scattered electron (BSE) image taken from the chosen sample area. The two particles in bright color on top left and bottom middle are galena particles, while the other particles are chalcopyrite particles. The lead element mapping of the sample was shown in Figure 5.10 (b). As can be seen, lead can only be detected on galena surface, indicating that there is no lead adsorbed on chalcopyrite surface. However, in the copper element mapping image shown in Figure 5.10 (c), copper can be observed not only on chalcopyrite surface, but also on galena surface. This proves that copper ions released from chalcopyrite can contaminate galena surface, which is responsible for the disappearance of the selective depressive effect of PAM in chalcopyrite-galena mixture flotation.



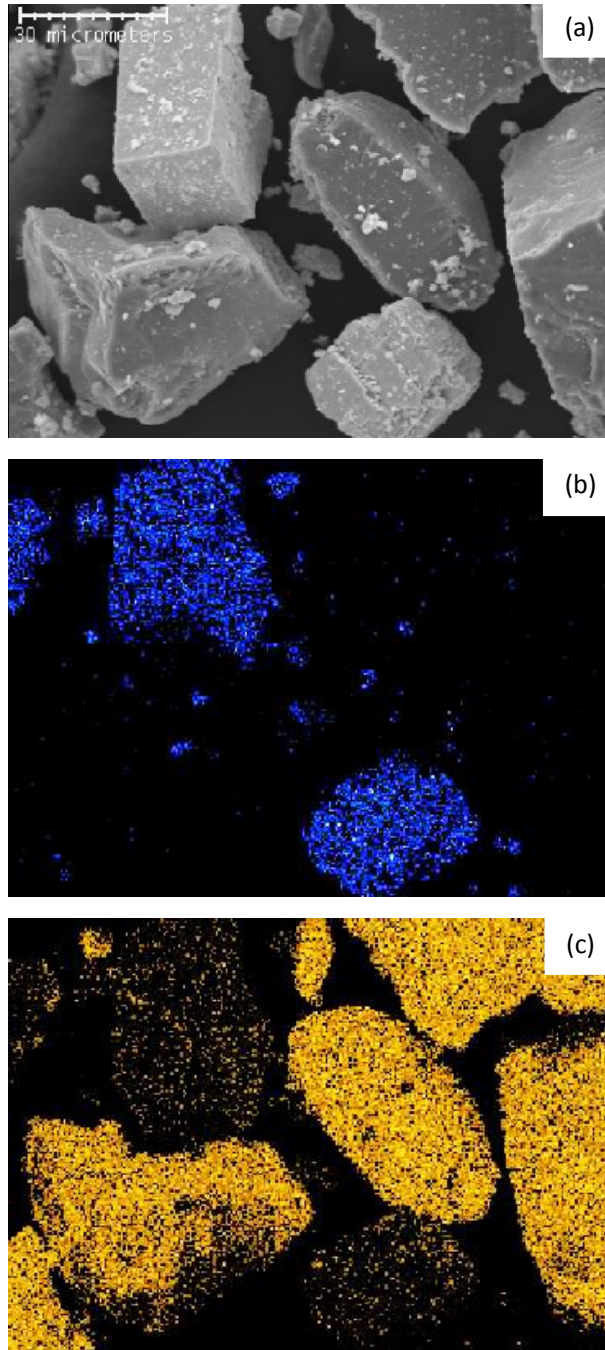


Figure 5.10 Energy-dispersive X-ray element mapping images of galena and chalcopyrite mixture: (a) grain BSE image of the mineral sample, (b) lead element mapping image, (c) copper element mapping image.

### *5.3.3 The Use of EDTA for Surface Cleaning*

EDTA has been chosen to remove the copper ions from galena surface. A simple experiment was designed to test the ability of EDTA to remove copper ions adsorbed on galena surface. In the experiment, 1 g -38  $\mu\text{m}$  galena and 1 g -150+75  $\mu\text{m}$  chalcopyrite were mixed in 100 mL distilled water. The suspension was adjusted to pH 10 and stirred for 10 minutes. Then the mineral mixture was filtered and screened by a 270 mesh sieve (53  $\mu\text{m}$  aperture). Thus, small sized galena and large sized chalcopyrite were separated. After separation, the fine galena was dried in a desiccator, and divided into two parts with the same weight. The first half was mixed with 100 mL solution containing 20 mg/L EDTA, and conditioned for 10 minutes, then filtered. The copper concentration in the filtrate was measured by atomic absorption spectroscopy (AAS), and the detected copper concentration was shown in Figure 5.11 as “EDTA solution”. The filter cake (i.e., galena after EDTA treatment), as well as the second half of the desiccator-dried galena (which was contacted with chalcopyrite but was not treated by EDTA) were separately treated by 0.1 M hydrochloric acid. After filtration, the HCl solutions were analyzed by the AAS to determine copper concentration. These are shown in Figure 5.11 as “Galena before EDTA” and “Galena after EDTA”, respectively. As can be seen, the fine galena after contacting the chalcopyrite released 0.165 ppm copper ions, whereas the same galena after EDTA treatment

released only 0.071 ppm copper ions. The difference, 0.094 ppm, was close to the copper ion concentration of the “EDTA solution” (0.112 ppm). The result shows that EDTA was able to remove most of the copper ions from galena surface. However, it can be seen that after EDTA treatment, galena still contains some copper. This means that EDTA cannot completely remove all the adsorbed copper on galena surface at the dosages tested.

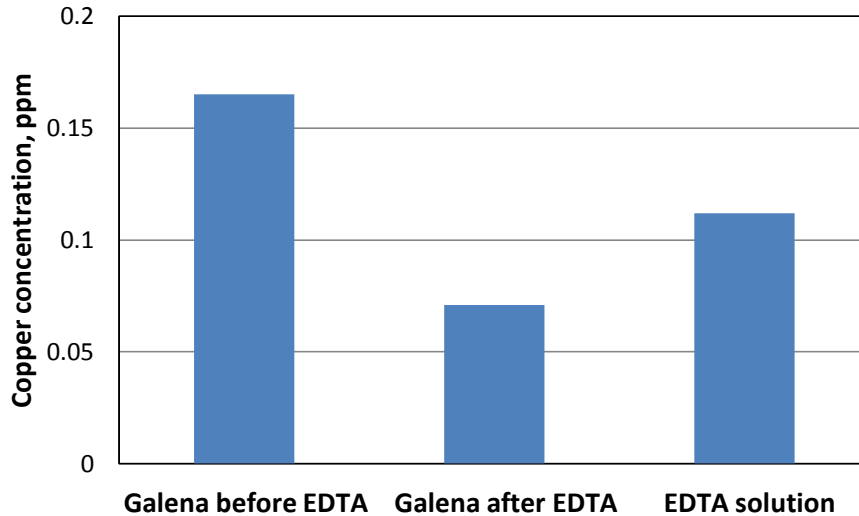


Figure 5.11 Copper ion concentration released from galena samples contacted with chalcopyrite, before and after EDTA treatment.

#### *5.3.4 Galena and Chalcopyrite Mixture Flotation with EDTA as a Cleaning Agent*

In galena and chalcopyrite mixture flotation, 20 mg/L EDTA has been added to slurry before the addition of PAM and KEX. Figure 5.12 (a) shows the flotation recovery and Figure 5.12 (b) shows the metal grade in flotation concentrate. The metal grade of the artificial mixtures before flotation is also shown in Figure 5.12 (a) for comparison. As the pH increased from 7 to 10, the recoveries of galena are relatively stable around 60%. The recovery of chalcopyrite was 11% at pH 7, then increased to the peak of 22% at pH 8.3, and dropped to 17% at pH 10. Overall, the separation between galena and chalcopyrite were not very sensitive to pH, while the optimum separation was at pH 7. However, it can be noted that the separation in mixture flotation was not as good as in single mineral flotation. The best separation achieved in single mineral flotation is a difference of 80 percentage points at pH 9, while in mixture flotation it is only 46 percentage points at pH 7. Galena has lower recovery in mineral mixture flotation than in single mineral flotation, which may be due to the residual copper adsorbed on galena surface. Meanwhile, chalcopyrite has higher recovery in mixture flotation than in single flotation. One possible explanation is that some fine chalcopyrite particles were flocculated with galena particles by the flocculating effect of PAM. Then these flocs floated into concentrate, increasing the recovery of the chalcopyrite.

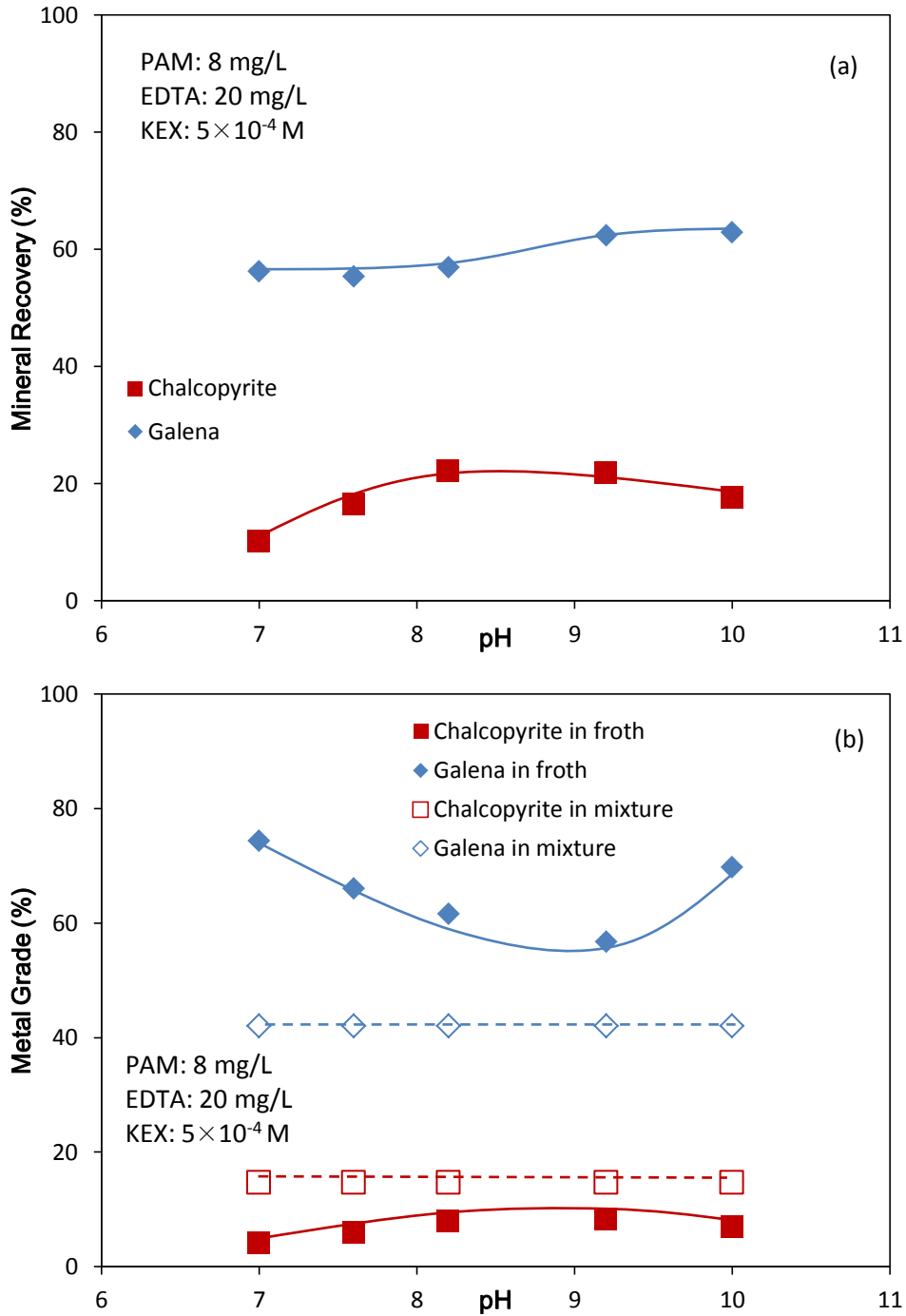


Figure 5.12 Flotation of chalcopyrite and galena mixture (weight ratio 1:1) with EDTA as a function of pH. (a) Metal recovery in froth product; (b) Metal grade in froth product. (EDTA: 20 mg/L; PAM: 8 mg/L; KEX:  $5 \times 10^{-4}$  mol/L; Flotation time: 5 min).

The effect of EDTA dosage was also investigated in mineral mixture flotation of galena and chalcopyrite, the result is shown in Figure 5.13. As can be seen, the optimum dosage is 20 mg/L. It is interesting to note that when the dosage of EDTA is increased to 60 mg/L, both galena and chalcopyrite were severely depressed. The reason for this phenomenon is not clear at this point.

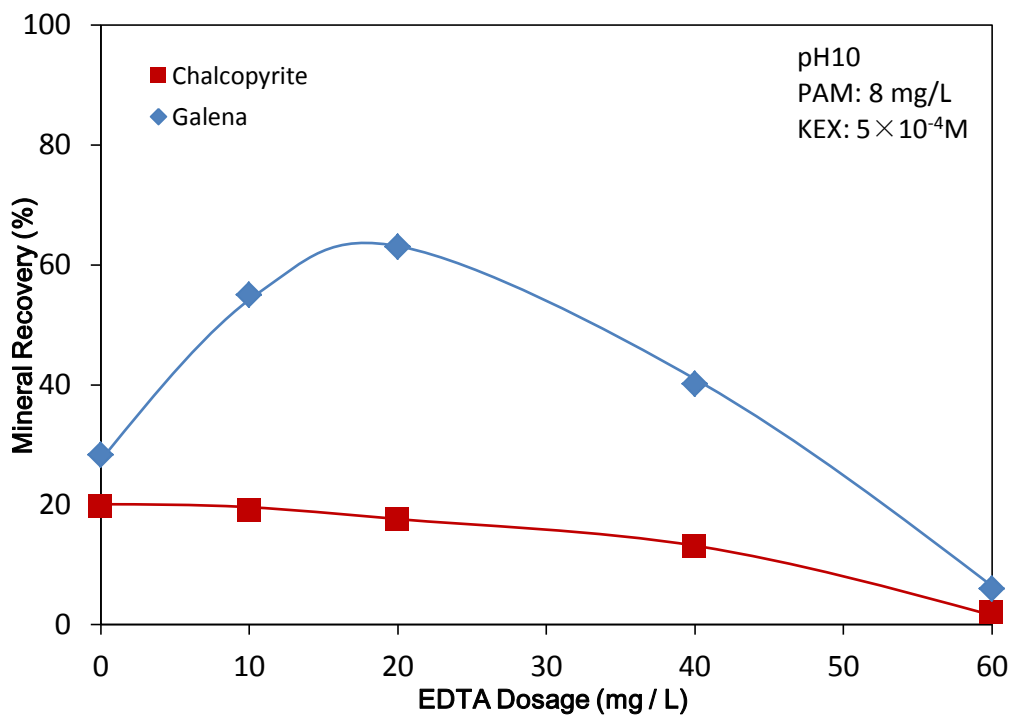


Figure 5.13 Flotation of the mixture of chalcopyrite and galena with EDTA as a function of EDTA dosage. (pH 10; PAM: 8 mg/L; KEX:  $5 \times 10^{-4}$  mol/L; Flotation time: 5 min).

### 5.3.5 ToF-SIMS Measurements

ToF-SIMS was employed to prove the surface cleaning effect of EDTA in galena and chalcopyrite mixture flotation. By determining metal ion and PAM distribution on the mineral surface, ToF-SIMS can also detect the possible selective adsorption of PAM on galena or chalcopyrite surfaces. After the measurements, the positive ion of  $\text{Cu}^+$  from the spectra was used to represent chalcopyrite distribution since chalcopyrite was the only source of  $\text{Cu}^+$ . Similarly, the positive ion of  $\text{Pb}^+$  was used to determine the distribution of galena in the mixture. The fragment of  $\text{C}_3\text{H}_5\text{NO}$ , as the monomeric unit of PAM, was used to show the distribution of PAM on the mineral mixture surface. On the ToF-SIMS images, the area with brighter color means higher intensity (concentration) of the selected ion.

Figure 5.14 (a), (b), (c) shows the distribution of chalcopyrite, galena and PAM without EDTA cleansing on a sample area of  $50\ \mu\text{m} \times 50\ \mu\text{m}$ . Figure 5.14 (a) and (b) shows that galena and chalcopyrite particles complement each other on sample area. Figure 5.14 (c) shows the distribution of PAM on mineral surface. By comparing these three images, it can be seen that PAM exist on both galena and chalcopyrite mineral surface, with similar intensity. This is consistent with the mixture flotation results (section 5.3.1) which show that without EDTA, PAM

depressed galena and chalcopyrite together.

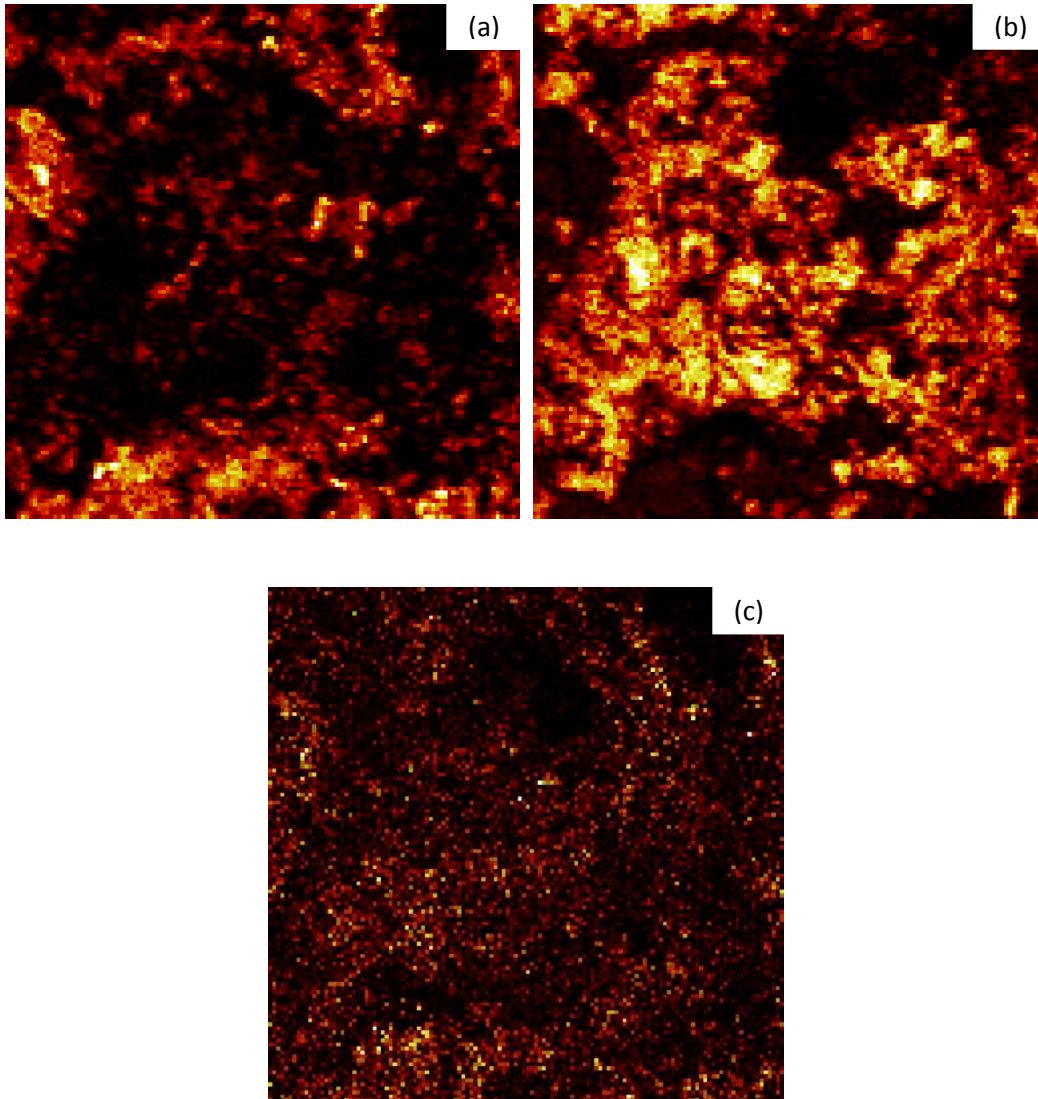


Figure 5.14 ToF-SIMS images 50 μm × 50 μm region of the surface of a mixture of chalcopyrite and galena after PAM and KEX treatment. (a) Image of chalcopyrite (Cu<sup>+</sup>); (b) Image of galena (Pb<sup>+</sup>); (c) Image of PAM (C<sub>3</sub>H<sub>5</sub>ON).



The ToF-SIMS measurements were then carried out on the mineral sample prepared with EDTA cleansing. The results were shown in Figure 5.15 (a), (b), (c). By comparing these three images, it is apparent that the brighter area in (c) matches exactly with the pattern of chalcopyrite distribution in (a), while the other area corresponding to galena is much darker. This suggests that, after adding EDTA, PAM has mostly adsorbed on chalcopyrite while very little on galena. It should be noted that low intensity PAM was still detected on galena surface, indicating that EDTA cannot remove copper ions completely from galena surface. This explains why the galena recovery in mineral mixture flotation after EDTA cleansing was still lower than that in single mineral flotation.

The comparison of the ToF-SIMS results before and after EDTA cleansing proves the surface cleaning effect of EDTA, which can remove the copper ions adsorbed on galena surface. It is also consistent with the previous conclusions from contact angle measurements and XPS measurements, that the combined use of PAM and KEX can make PAM selectively adsorb on chalcopyrite but not galena.

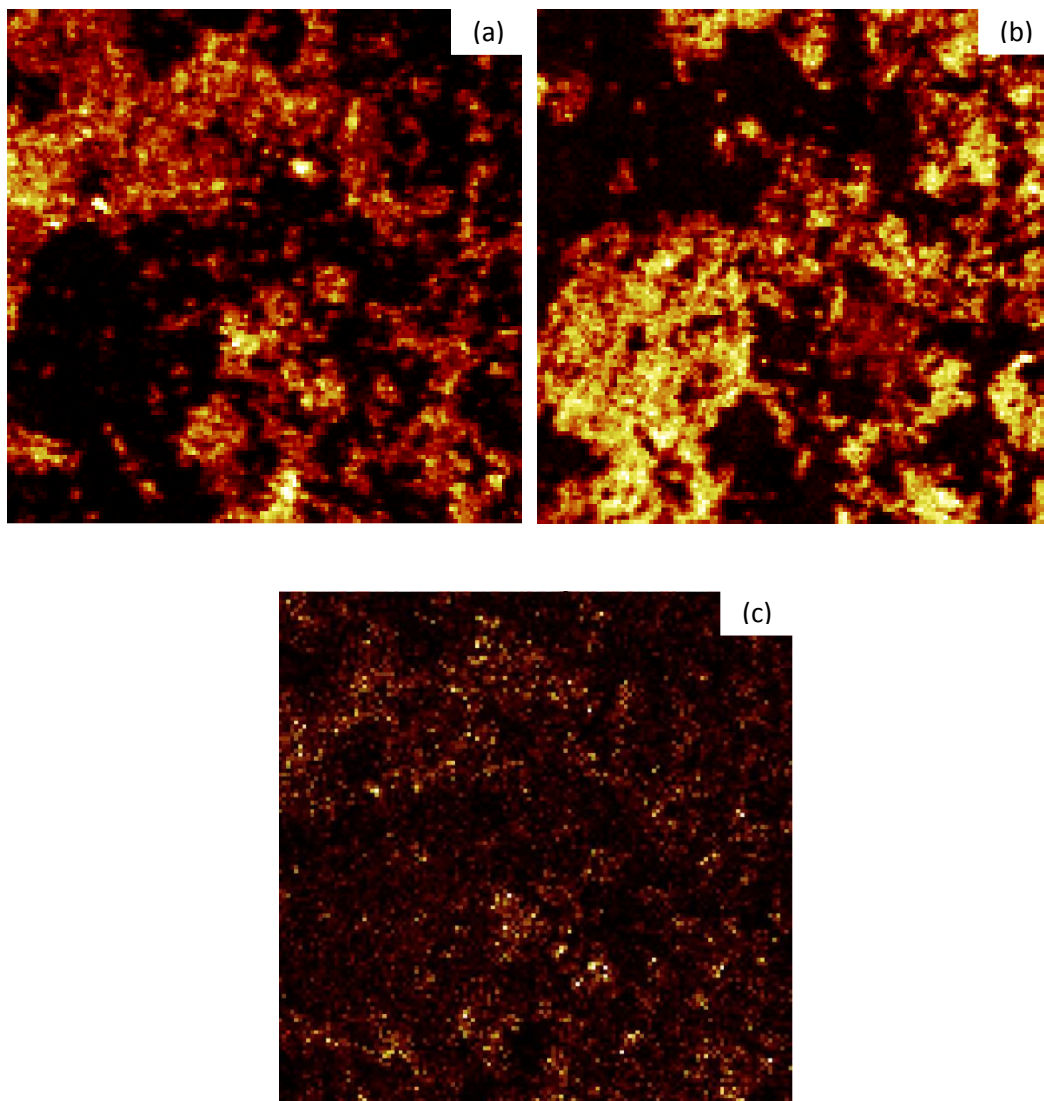


Figure 5.15 ToF-SIMS images of  $50\ \mu\text{m} \times 50\ \mu\text{m}$  region of the surface of a mixture of chalcopyrite and galena after EDTA cleaning and PAM and KEX treatment. (a) Image of chalcopyrite ( $\text{Cu}^+$ ); (b) Image of galena ( $\text{Pb}^+$ ); (c) Image of PAM ( $\text{C}_3\text{H}_5\text{ON}$ ).

## 6. CONCLUSIONS AND RECOMMENDATIONS

### 6.1 General Findings

1. In single sulfide mineral flotation with KEX as a collector, PAM (8 mg/L) can depress chalcopyrite, pyrite and sphalerite, but not galena in the pH range from 9 to 11. The recovery difference between galena and chalcopyrite is up to 80 percentage points.
2. The zeta potential measurements show that the selective depressive effect of PAM on galena and chalcopyrite is not caused by the electrostatic interaction.
3. The contact angle measurements indicate that PAM can adsorb on both galena and chalcopyrite surface to lower their hydrophobicity. The addition of KEX after PAM can restore the surface hydrophobicity of galena, while chalcopyrite surface remains relatively hydrophilic. The use of PAM and KEX together gives the separation window in galena and chalcopyrite single mineral flotation.
4. In XPS measurements, amide groups and ammonium groups can be detected on the surface of chalcopyrite after PAM adsorption, while only amide groups were observed on galena. After adding KEX, amide and ammonium peaks on

chalcopyrite did not change but the amide peak on galena disappeared. The adsorption of PAM on galena is only through hydrogen bonding, while on chalcopyrite involves hydrogen bonding as well as chemical complexation. Chalcopyrite-PAM bonding is stronger than galena-PAM bonding, since only the latter can be broken up by KEX.

5. There is no separation in the mixture flotation of galena and chalcopyrite without adding EDTA. Both galena and chalcopyrite are floated in low PAM dosage under 2 mg/L, and both are depressed in high PAM dosage above 4 mg/L at pH 10.
6. In X-ray mapping experiment, copper can be detected on galena surface while no lead can be seen on chalcopyrite surface. The copper ions released from chalcopyrite adsorb on galena surface, caused the disappearance of the selectivity of PAM.
7. EDTA shows the ability to remove the adsorbed copper ions on galena surface, although there are still some residual copper on galena after EDTA treatment at the dosage tested.
8. With EDTA added as a cleaning agent, galena and chalcopyrite can be separated by PAM and KEX. The best separation happens at pH 7 with a 46%

recovery difference. The separation is not sensitive to pH change in the pH range from 7 to 10. The optimum EDTA dosage is 20 mg/L. At high EDTA dosages, both galena and chalcopyrite are severely depressed.

9. ToF-SIMS measurements illustrate that before EDTA treatment PAM adsorbs on both galena and chalcopyrite surface, while after EDTA treatment PAM mainly adsorbs on chalcopyrite surface.

## **6.2 Recommendations for Future Work**

1. The current research mainly focused on the selective depressive effect of PAM on galena and chalcopyrite. The other important advantage of using PAM as a depressant, which is the selective flocculation effect, has not been systematically studied. Mineral mixture flotation with particles size  $-38\ \mu\text{m}$  or  $-25\ \mu\text{m}$ , and techniques like Photometric Dispersion Analyzer could be employed to examine the dual functions of PAM as both a flocculant and a selective depressant for fine galena and chalcopyrite mineral particles.
2. All the flotation tests were conducted by small-scale flotation tube with artificial mineral mixture. Future study should scale-up to batch flotation by using natural ore samples.

3. The PAM used in the research is non-ionic without any modification. Since the characteristics of PAM will vary by its charge, hydrolysis and grafting, the use of anionic PAM, partially hydrolyzed PAM or PAM with other substituted functional groups might improve the separation.

## BIBLIOGRAPHY

Ahmed, N., and Jameson, G. (1985). The effect of bubble size on the rate of flotation of fine particles. *International Journal of Mineral Processing*, 14(3), 195-215.

Allan, W., Bourke, R.D. (1978). Mattabi mines ltd. milling practice in Canada. In: Pickett, E. (Ed.), *CIM Special*. 16, 175-177.

Barvenik, F. W. (1994). Polyacrylamide characteristics related to soil applications. *Soil Science*, 158(4), 235.

Boulton, A., Fornasiero, D., and Ralston, J. (2001). Selective depression of pyrite with polyacrylamide polymers. *International Journal of Mineral Processing*, 61(1), 13-22.

Bulatovic, S. M. (2007). *Handbook of Flotation Reagents - Chemistry, Theory and Practice, Volume 2 - Flotation of Sulfides Ores*: Elsevier.

C.-Y. Lu, B., and Graydon, W. F. (1955). Rates of Copper Dissolution in Aqueous Ammonium Hydroxide Solutions<sup>1</sup>. *Journal of the American Chemical Society*,

77(23), 6136-6139.

Cebeci, Y. (2003). Investigation of kinetics of agglomerate growth in oil agglomeration process. *Fuel*, 82(13), 1645-1651.

Chandra, A., and Gerson, A. (2009). A review of the fundamental studies of the copper activation mechanisms for selective flotation of the sulfide minerals, sphalerite and pyrite. *Advances in colloid and interface science*, 145(1), 97-110.

Daughton, C. G. (1988). Quantitation of acrylamide (and polyacrylamide): critical review of methods for trace determination/formulation analysis and future-research recommendations: California Public Health Foundation.

Dudnikov, S. V., and Galikov, A.A. (1969). *Theory and Practice of Application of Flotation Reagents*.

Fuerstenau, C. F., Miller, J.D., Pray, R.E. and Perinne, B.F. (1965). Metal ion activation in xanthate flotation of quartz. *Trans. AIME*, 232, 359.

Fuerstenau, M. C., Harper, R.W. and Miller, J.D. (1970). Hydroxamate vs. fatty acid flotation of iron oxide. *Trans. AIME.*, 247, 69-73.



Gong, J. (2011). The Role of High Molecular Weight Polyethylene Oxide in Reducing Quartz Gangue Entrainment in Chalcopyrite Flotation by Xanthate Collectors. Doctoral dissertation, University of Alberta.

Gong, J., Peng, Y., Bouajila, A., Ourriban, M., Yeung, A., and Liu, Q. (2010). Reducing quartz gangue entrainment in sulphide ore flotation by high molecular weight polyethylene oxide. *International Journal of Mineral Processing*, 97(1), 44-51.

Green, V. S., and Stott, D. (1999). Polyacrylamide: A review of the use, effectiveness, and cost of a soil erosion control amendment. Paper presented at the Selected papers from the 10th International Soil Conservation Organization Meeting held May.

Griot, O., and Kitchener, J. (1965). Role of surface silanol groups in the flocculation of silica suspensions by polyacrylamide. Part 1.—Chemistry of the adsorption process. *Transactions of the Faraday Society*, 61, 1026-1031.

Guy, P., and Trahar, W. (1984). The effects of oxidation and mineral interaction on sulphide flotation. *Flotation of sulphide minerals*, 91-110.

Halpern, J. (1953). Kinetics of the dissolution of copper in aqueous ammonia. *Journal of the Electrochemical Society*, 100(10), 421-428.

Hantsche, H. (1993). High resolution XPS of organic polymers, the scienta ESCA300 database. By G. Beamson and D. Briggs, Wiley, Chichester 1992. *Advanced Materials*, 5(10), 778-778.

Hong, P. K. A., Li, C., Banerji, S. K., and Regmi, T. (1999). Extraction, recovery, and biostability of EDTA for remediation of heavy metal-contaminated soil. *Journal of soil contamination*, 8(1), 81-103.

Huang, P., Cao, M., and Liu, Q. (2012a). Using chitosan as a selective depressant in the differential flotation of Cu–Pb sulfides. *International Journal of Mineral Processing*, 106, 8-15.

Huang, P., Cao, M., and Liu, Q. (2012b). Adsorption of chitosan on chalcopyrite and galena from aqueous suspensions. *Colloids and Surfaces A: Physicochemical and Engineering Aspects*.

Johnson, N. W., Mckee, D.J. and Lynch, A.J. (1974). *Trans. AIME*, 256, 204-226.

Kelebek, S., and Smith, G. W. (1989). Electrokinetic properties of a galena and chalcopyrite with the collectorless flotation behaviour. *Colloids and Surfaces*, 40(1-2), 137-143.

King, R. P. (1982). *Principles of flotation* South African Institute of Mining and Metallurgy, Kelvin House, 2 Holland St, Johannesburg, South Africa.

Laskowski, J., Liu, Q., and Zhan, Y. (1997). Sphalerite activation: flotation and electrokinetic studies. *Minerals Engineering*, 10(8), 787-802.

Laskowski, J. S., Liu, Q., and Bolin, N. J. (1991). Polysaccharides in flotation of sulphides. Part I. Adsorption of polysaccharides onto mineral surfaces. *International Journal of Mineral Processing*, 33(1-4), 223-234.

Lin, K., and Burdick, C. (1988). *Polymeric depressants*. Marcel Dekker, Inc., *Reagents in Mineral Technology*, 471-483.

Lindberg, B., Maripuu, R., Siegbahn, K., Larsson, R., Gölander, C. G., and Eriksson, J. C. (1983). ESCA Studies of heparinized and related surfaces: 1. Model surfaces on steel substrates. *Journal of Colloid and Interface Science*, 95(2), 308-321.

Linke, W. F., and Booth, R. B. (1960). Physical chemical aspects of flocculation by polymers. Transactions of the American Institute of Mining and Metallurgical Engineers, 217, 364-371.

Lipp, D., and Kozakiewicz, J. (1991). Acrylamide polymers. Kirk-Othmer Encyclopedia of Chemical Technology.

Liu, C. (1982). Separating copper-lead concentrate by flotation with sodium pyrophosphate. Yu Se Chin Shu, 34(1), 593–600.

Liu, G., Zhong, H., Hu, Y., Zhao, S., and Xia, L. (2007). The role of cationic polyacrylamide in the reverse flotation of diasporic bauxite. Minerals Engineering, 20(13), 1191-1199.

Liu, Q. (2012). Selective aggregation of hydrophilic gangue minerals in froth flotation. MRS Proceedings, Cambridge Univ Press.

Liu, Q., and Laskowski, J. (1989a). The interactions between dextrin and metal hydroxides in aqueous solutions.

Liu, Q., and Laskowski, J. S. (1989b). The role of metal hydroxides at mineral

surfaces in dextrin adsorption, II. Chalcopyrite-galena separations in the presence of dextrin. *International Journal of Mineral Processing*, 27(1–2), 147-155.

Liu, Q., Wannas, D., and Peng, Y. (2006). Exploiting the dual functions of polymer depressants in fine particle flotation. *International Journal of Mineral Processing*, 80(2–4), 244-254.

Lovell, V. M. (1982). Industrial flotation reagents. In: King, R.P. (ED.), *Principles of Flotation*. Institute of Mining and Metallurgy.

McQuiston, F. W. (1957). Flotation of Complex Copper - lead zinc ores. *Progress in Mineral Dressing IMPC*, 3, 511-519.

Meng, X., and Kenneth, N. (1996). The principles and applications of ammonia leaching of metals—a review. *Mineral Processing and Extractive Metallurgy Review*, 16(1), 23-61.

Michaels, A., and Morelos, O. (1955). Polyelectrolyte adsorption by kaolinite. *Industrial and Engineering Chemistry*, 47(9), 1801-1809.

Moody, G. (1992). The use of polyacrylamides in mineral processing. *Minerals*

Engineering, 5(3-5), 479-492.

Morel, F. M. M. (1983). Principles of aquatic chemistry. John Wiley and Sons, New York NY. 1983. 446.

Mortimer, D. A. (1991). Synthetic polyelectrolytes—a review. Polymer international, 25(1), 29-41.

Moudgil, B. M. (1983). Effect of polyacrylamide and polyethylene oxide polymers on coal flotation. Colloids and Surfaces, 8(2), 225-228.

Neethling, S., and Cilliers, J. (2001). Simulation of the effect of froth washing on flotation performance. Chemical engineering science, 56(21), 6303-6311.

Pradip, Y. A. A., and Fuerstenau, D. W. (1980). The adsorption of polyacrylamide flocculants on apatites. Colloid and Polymer Science, 258(12), 1343-1353.

Qin, W., Wei, Q., Jiao, F., Li, N., Wang, P., and Ke, L. (2012). Effect of sodium pyrophosphate on the flotation separation of chalcopyrite from galena. International Journal of Mining Science and Technology, 22(3), 345-349.

Rao, M. K. Y., and Natarajan, K. A. (1990). Effect of electrochemical interactions among sulfide minerals and grinding medium on the flotation of sphalerite and galena. [Article]. *International Journal of Mineral Processing*, 29(3-4), 175-194.

Read, A. D. (1971). *Trans. IMM*, 80(C), 24 - 31.

Roberts, A., Burns, C., and Cameron, A. (1980). Metallurgical Development at Woodlawn Mines, Australia. *Complex Sulphide Ores*, 128-134.

Rubio, J., and Hoberg, H. (1993). The process of separation of fine mineral particles by flotation with hydrophobic polymeric carrier. *International Journal of Mineral Processing*, 37(1-2), 109-122.

Schnarr, J. R. (1978). Brunswick mining and smelting corporation. Milling practice in Canada. In: Pickett, D.E. (Ed.), *CIM Special*, 16, 158 - 161.

Senior, G. D., and Trahar, W. J. (1991). The influence of metal hydroxides and collector on the flotation of chalcopyrite. *International Journal of Mineral Processing*, 33(1-4), 321-341.

Seybold, C. A. (1994). Polyacrylamide review: Soil conditioning and

environmental fate. [Article]. *Communications in Soil Science and Plant Analysis*, 25(11-12), 2171-2185.

Shimoiizaka, J., Usui, S., Matsuoka, I. and Sasaki, H. (1976). Depression of galena flotation by sulfite and chromiumion. In: M.C. Fuerstenau (Editor). *Flotation - A.M. Gaudin Memorial Volume*. AIME, New York, NY,, 393-413.

Singh, R., Subba Rao, S., Maulik, S., and Chakravorty, N. (1997). Fine particles flotation-Recent trends. *Transactions of the Indian Institute of Metals*, 50(5), 407-419.

Sivamohan, R. (1990). The problem of recovering very fine particles in mineral processing — A review. *International Journal of Mineral Processing*, 28(3-4), 247-288.

Siwek, B., Zembala, M., and Pomianowski, A. (1981). A method for determination of fine-particle flotability. [Note]. *International Journal of Mineral Processing*, 8(1), 85-88.

Sojka, R., and Lentz, R. (1994). Polyacrylamide (PAM): A new weapon in the fight against irrigation-induced erosion. *USDA-ARS Soil and Water Management*



Research Unit: Station Note.

Song, S., Lopez-Valdivieso, A., Reyes-Bahena, J., and Lara-Valenzuela, C. (2001). Floc flotation of galena and sphalerite fines. *Minerals Engineering*, 14(1), 87-98.

Sönmez, İ., and Cebeci, Y. (2003). Fundamental aspects of spherical oil agglomeration of calcite. *Colloids and Surfaces A: Physicochemical and Engineering Aspects*, 225(1), 111-118.

Subrahmanyam, T. V., and Forssberg, K. S. E. (1990). Fine particles processing: shear-flocculation and carrier flotation — a review. *International Journal of Mineral Processing*, 30(3–4), 265-286.

Sui, C., Brienne, S., Ramachandra Rao, S., Xu, Z., and Finch, J. (1995). Metal ion production and transfer between sulphide minerals. *Minerals Engineering*, 8(12), 1523-1539.

Trahar, W. (1981). A rational interpretation of the role of particle size in flotation. *International Journal of Mineral Processing*, 8(4), 289-327.

Trahar, W., and Warren, L. (1976). The flotability of very fine particles—A review.

International Journal of Mineral Processing, 3(2), 103-131.

Uchida, E., Uyama, Y., Iwata, H., and Ikada, Y. (1990). XPS analysis of the poly (ethylene terephthalate) film grafted with acrylamide. Journal of Polymer Science Part a-Polymer Chemistry, 28(10), 2837-2844.

Wagner, C. D., Naumkin, A.V., Kraut-Vass, A., Alisson, J.W., Powell, C.J., Rumble, J.R.Jr. (2003). NIST-X-ray Photoelectron Spectroscopy Database 20 Version 3.4. National Institute of Standards and Technology, Gaithersburg, MD.

Wang, K., Wang, L., Cao, M., and Liu, Q. (2012). Xanthation-modified polyacrylamide and spectroscopic investigation of its adsorption onto mineral surfaces. Minerals Engineering, 39(0), 1-8.

Wang, X. H., and Forssberg, E. (1990). EDTA-induced flotation of sulfide minerals. [Article]. Journal of Colloid and Interface Science, 140(1), 217-226.

Warren, L. J. (1975). Shear-flocculation of ultrafine scheelite in sodium oleate solutions. Journal of Colloid and Interface Science, 50(2), 307-318.

Warren, L. J. (1984). Principles of Mineral Flotation (M.N. Jones and J.T.

Woodcock, Eds.). The Australian Institute of Mining and Metallurgy, 185-214.

Webster's-online-dictionary. Froth flotation, [www.websters-online-dictionary.org](http://www.websters-online-dictionary.org).

Zhang, J., Hu, Y., Wang, D., and Xu, J. (2004). Depressing effect of hydroxamic polyacrylamide on pyrite. *Journal of Central South University of Technology*, 11(4), 380-384.